

Characterization of Crn7, a novel mammalian Golgi protein

INAUGURAL-DISSERTATION
zur
Erlangung des Doktorgrades
der Mathematisch-Naturwissenschaftlichen Fakultät
der Universität zu Köln



vorgelegt von

Vasily RYBAKIN

aus
St. Petersburg, Russland

Köln, 2005

Referees/Berichterstatter:

Prof. Dr. Angelika A. Noegel
Prof. Dr. Karin Schnetz

Date of oral examination:

(Tag der mündlichen Prüfung)

02/12/2005

The present research work was carried out under the supervision of Prof. Dr. Angelika A. Noegel, in the Institute of Biochemistry I, Medical Faculty, University of Cologne (Cologne, Germany) from May 2003 to September 2005.

Diese Arbeit wurde von April 2003 bis September 2005 am Biochemischen Institut I der Medizinischen Fakultät der Universität zu Köln unter der Leitung von Prof. Dr. Angelika A. Noegel durchgeführt.

Hamauue

OO. CONTENTS.

O. Opening remarks	5
1. Introduction	6
1.1. Coronin proteins as actin regulators	10
1.1.1. Yeast coronin regulates the actin cytoskeleton by directly interacting with Arp2/3 complex	11
1.1.2. <i>Drosophila</i> Dpod1: An actin-tubulin linker regulating the development of the nervous system	13
1.1.3. Mammalian short coronins and the actin cytoskeleton	14
1.2. Coronin and POD-1 proteins at the interface of cytoskeleton and trafficking	18
1.2.1. <i>Drosophila</i> coro possibly acts as a linker between the actin cytoskeleton and membrane transport	19
1.2.2. <i>C. elegans</i> POD-1, an actin-binding protein participating in vesicular trafficking	20
1.3. Mammalian coronins with unexplored functions	21
1.4. Clinical implications	22
2. Aims of the work	25
3. Results	26
3.1. Crn7 sequence analysis	26
3.2. Tissue distribution and developmental dynamics of Crn7	29
3.3. Subcellular localization of Crn7	31
3.3.1. Crn7 is present in the cis-Golgi and in the cytosol	31
3.3.2. Crn7 is localized to the outer side of Golgi membranes	35
3.3.3. Stabile association of Crn7 with the Golgi requires the integrity of ER-to-Golgi transport	36
3.3.4. Properties of cytosolic and membrane-associated forms of Crn7	39
3.4. Analysis of Crn7 function by RNAi	40
3.4.1. Use of siRNA duplexes to silence Crn7	40
3.4.2. Influence of Crn7 RNAi on the Golgi architecture	42
3.4.3. Block of protein export from the Golgi in Crn7 RNAi cells	44
4. Discussion	51
4.1. Physical structure and inheritance of the Golgi complex	51
4.2. Protein import and progression in the Golgi	54
4.3. Golgi export	55
4.4. Models of Golgi dynamics	57
4.5. Crn7 is a novel WD-repeat protein localized to the Golgi complex	59
4.6. Targeting of Crn7 to the Golgi	60
4.7. Possible function of Crn7 in the Golgi complex	62
4.8. Crn7 is an essential mammalian protein.	63
5. Materials and methods	65
6. Abbreviations	72
7. Literature	73
Abstracts (English/German)	80
Erklärung	82
Curriculum vitae	83
Lebenslauf	84

O. OPENING REMARKS

This work would never have been accomplished without constant help and support from my friends and colleagues. I am deeply grateful to Prof. Angelika A. Noegel for offering me the opportunity to perform my PhD work in her lab. Rainer Duden and Irina Majoul (Cambridge - London), Maria Stumpf, Rolf Müller, Andreas Hasse (Cologne) and Dharamdajal Kalicharan (Groningen) patiently taught me methods and helped with experiments. My quite part-time co-bosses Andreas Hasse and Christoph Clemen *sometimes* popped up with valuable comments. Akis Karakesisoglu, Deen Bakthavatsalam, Rainer Duden, Irina Majoul and Stefan Höning read piles of paper I brought along and even tolerated questions. Bettina Lauss, Dörte Püsche and Budi Tunggal (Cologne) are acknowledged for expert administrative support.

I am grateful to all colleagues of mine who openly, and sometimes too frankly (*mind the understatement*) shared their opinions about my work during scientific meetings and conferences in Barcelona, Annaberg, Washington and Cologne, and for sharing key chemicals. The people in the lab (Soraya, Christoph, Thorsten, Carola, Maria, Yogi, Deen, Wenshu, Sabu, Jessica, Andreas, Kumar, Berthold, Budi, Ria, Martina, Hua, Hafi, Rolf, “Kletten”-André, Christian, Marion, “Commandante” Akis, Maria, Francisco, Gudrun and *especially* Rosi) made my life here pleasant and *definitely* not boring.

I am especially thankful to Natasha Gounko (Groningen) for her support, advise and help.
Спасибо, рыжик!

Kölsch is not beer. *At all.*

1. INTRODUCTION

Coronins constitute an evolutionarily conserved family of WD-repeat actin-binding proteins, which can be clearly classified into two distinct groups based on their structural features. All coronins possess a conserved basic N-terminal motif and three to ten WD repeats clustered in one or two core domains. Dictyostelium and mammalian coronins are important regulators of the actin cytoskeleton, while the fly Dpod1 and the yeast coronin proteins crosslink both actin and microtubules. Apart from that, several coronins have been shown to be involved in vesicular transport. C. elegans POD-1 and Drosophila coro regulate the actin cytoskeleton, but also govern vesicular trafficking as indicated by mutant phenotypes. In both organisms, defects in cytoskeleton and trafficking lead to severe developmental defects ranging from abnormal cell division to aberrant formation of morphogen gradients.

WD-repeat (WD-40-domain-repeat) proteins are defined by the presence of at least four WD repeats located centrally in the protein. These repeats were discovered in 1986 (Fong et al., 1986) and are defined by a partially conserved domain of 40–60 amino acids starting with a glycine-histidine (GH) dipeptide 11–24 residues away from the N-terminus and ending with a tryptophane-aspartic acid (WD) dipeptide at the C terminus. The WD domain has no intrinsic catalytic activity and is thought to serve as a stable platform for simultaneous interactions with other proteins.

WD-repeat proteins have extremely diversified cellular functions. They play central roles in a variety of cellular events including, but not limited to, signal transduction, transcriptional regulation, remodeling the cytoskeleton and regulating vesicular trafficking. Several WD-repeat proteins have been linked to human diseases (Li and Roberts, 2001).

Coronin proteins constitute one of the more than thirty subfamilies (Yu et al., 2000) among the WD-repeat proteins and contain three to five clustered WD repeats forming the characteristic coronin core domain (de Hostos, 1999; Neer and Smith, 1996). Apart from the core domain, common structural features include a short conserved N-terminal motif and a 70 amino acid-region located C-terminally to the WD repeats. Furthermore, each coronin contains a unique, divergent region of about 100 amino acids, which follows the conserved C-terminal extension. This sequence may confer specific functions to any individual coronin protein while, in contrast, it differs between the species. A second region of variability is present in the fourth β -strand of the third WD repeat (de Hostos, 1999).

The first coronin protein was identified in *Dictyostelium discoideum* (de Hostos et al., 1991). Its name resulted from the location in the actin-rich crown-shaped cell surface projections. The *Dictyostelium* protein was indirectly shown to participate in the regulation of the actin cytoskeleton and vesicular trafficking. Early findings on structures and functions of coronin proteins, especially that of *Dictyostelium*, have been reviewed (de Hostos, 1999, see also A. Schulze, Diploma thesis, University of Cologne, 2001). Meanwhile, more than 20 coronins have been identified in vertebrates and invertebrates (de Hostos, 1999; Okumura et al., 1998). In mice and men, the coronin family of proteins comprises at least seven members (Table 1).

Most mammalian representatives typically demonstrate tissue-specific distribution patterns, whereas some are rather ubiquitous. Coronin 3 is the most-widely expressed mammalian member (Iizaka et al., 2000; Okumura et al., 1998; Spoerl et al., 2002). Coronin proteins clearly form two distinct subfamilies, short “conventional” coronins and longer proteins, respectively (Fig. 1). The first subfamily consists of approximately 450–650 amino acid proteins harboring a very carboxy-terminal coiled-coil region of 30–40 amino acids mediating homophilic dimerization and/or oligomerization of coronins (Asano et al., 2001; Spoerl et al., 2002), whereas

the second subfamily contains the closely related mammalian Crn7 and *C. elegans* and *Drosophila* POD-1 proteins, which are clearly distinct from the first group in that they possess two core domains rather than one.

coronin	synonyms	protein	accession #	main tissue expression	references
1	coronin 1A, clabp, clipinA, TACO, p57	461 aa	NP_009005	thymus, spleen, bone marrow, lymph nodes, peripheral leukocytes	(Okumura et al., 1998; Suzuki et al., 1995)
2	coronin 1B, coronin _{se} , p66	489 aa	NP_065174	gastrointestinal mucosa, liver, spleen, kidney, lung	(Parente et al., 1999)
3	coronin 1C, CORO1C	474 aa	NP_055140	Brain, lung, intestine, kidney	(Hasse et al., 2005; Iizaka et al., 2000; Spoerl et al., 2002)
4	coronin 2A, clipinB , IR10	525	NP_438171	colon, prostate, testis, brain, lung, epidermis	(Nakamura et al., 1999; Okumura et al., 1998; Zaphiropoulos and Toftgard, 1996)
5	coronin 2B, clipinC	475	NP_006082	brain	(Nakamura et al., 1999)
6	ClipinE 3 splicing variants	471 aa 431 aa	NP_624354,6 NP_624355	brain	NP_624354–6
7	Crn7	925 aa	NP_078811	ubiquitous	(Rybakin et al., 2004), this work

Table 1. Summary of the mammalian coronin proteins, their nomenclature, sizes, and major expression sites.

A recently discovered novel *Dictyostelium* long coronin/POD-1 homologue (A. A. Noegel and F. Rivero, personal communication) is also classified into the same subfamily. It is important to note that all known coronins belonging to the second group lack coiled-coil domains. However, harboring two core domains, longer coronin proteins may indeed be considered dimers with regard to the core domain functions.

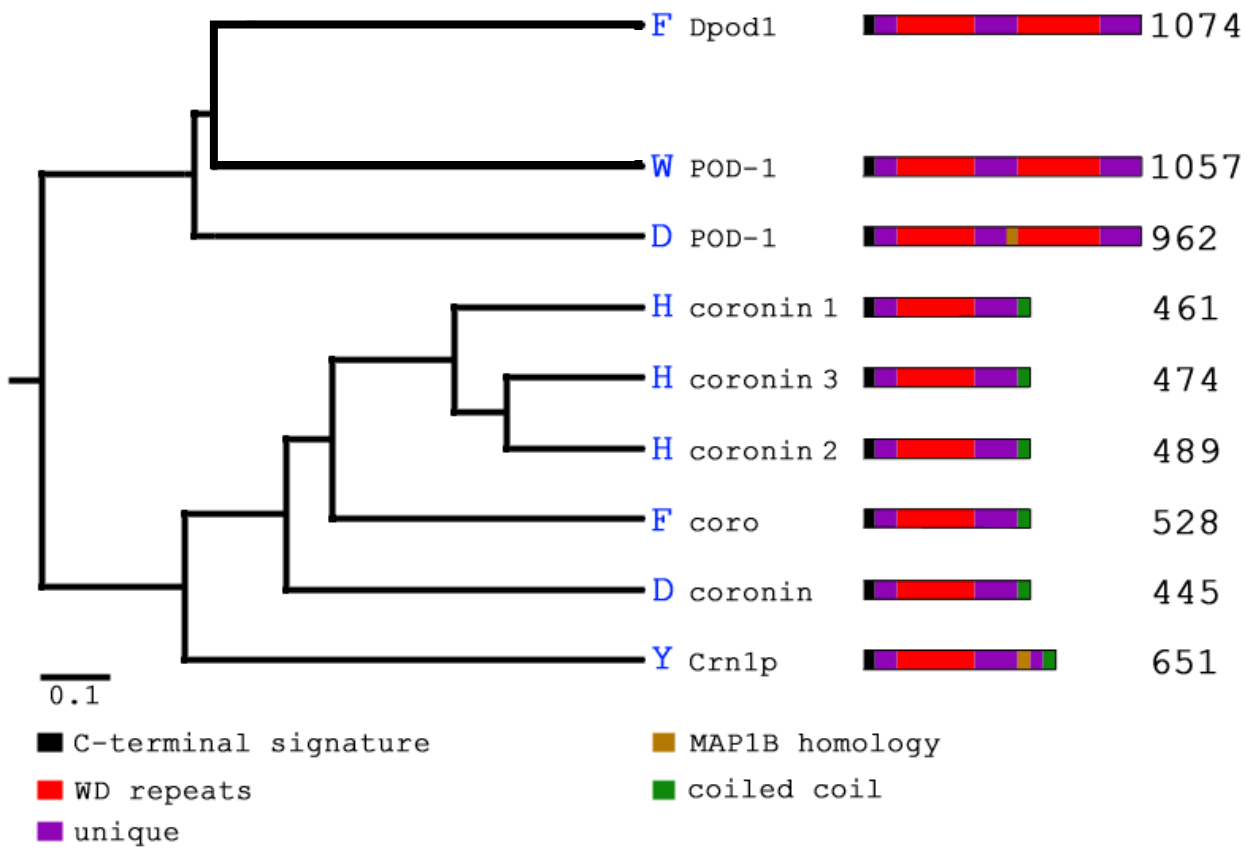


*Fig. 1. Comparison of domain structures of representative coronins and POD-1 proteins and their phylogenetic relationships. Phylogenetic analysis was performed using ClustalW algorithm (European Bioinformatics Institute, Hinxton, UK), and the phylogenetic tree was build using the Phylodendron server at the University of Indiana, Bloomington, IN. Right to the phylogram, abbreviations indicating organisms, and protein names are given: F, *Drosophila melanogaster*; H, *Homo sapiens*; W, *Caenorhabditis elegans*; D, *Dictyostelium discoideum*; Y, *Saccharomyces cerevisiae*. On the right, domain structures and amino acid numbers for each protein are given.*

All known short coronins are characterized by the presence of an extremely highly basic N-terminal 12-amino acid motif (pI 12.5 for human coronin 1), which can be taken as a novel coronin signature (Table 2A), as it is only present in coronin proteins. In the longer coronins, this

sequence is reduced to a 5-amino acid core motif (Table 2B) that appears in front of each coronin core domain. A recent study suggests that this coronin signature is involved in actin binding (Oku et al., 2003), although this sequence is also present in coronin proteins that have not been associated with the actin cytoskeleton.

A	
D coronin	1 ms kvvvrsskyrhvfaaqpkk 20
H coronin 1	1 ms rqvvvrsskfrhvfgqpak 20
H coronin 3	1 mr rvvrqskfrhvfgqavkn 20
F coro	1 ms frvvrsskfrhvyygqalk 20
Y crnlp	1 msg kfvraskyrvhvfgqaak 20
B	
W POD-1 (1)	1 mawrffaa skfknttpkvpkk 20
W POD-1 (2)	551 gqits skfrhvdgqqgatksga 570
F Dpod1 (1)	1 mawrfka skyknAAPIVPKA 20
F Dpod1 (2)	611 stvfgkv skfrhlkgtpghk 630
D POD-1 (1)	1 mfkv skyrh tvgkidkrelw 20
D POD-1 (2)	482 givpkvvrs skyrhisgsa 500

Table 2. Coronin signatures present in short and long coronins. A, short coronins contain a stretch of 12 conserved basic amino acids at the very N-terminus. B, long coronins / POD-1 proteins harbor two copies of a 5-amino acid degenerated core signature at the N-terminus and in the intermediate region. Identical amino acids are indicated in red, similar amino acids in blue. Single-letter organism abbreviations as in Fig. 1.

1.1. Coronin proteins as actin regulators

Actin is one of the most-abundant cellular proteins executing multiple structural and regulatory functions (Cvrckova et al., 2004). The protein is conserved and ubiquitous, and exists

in α , β - and γ -isoforms in mammals. Monomeric actin (G-actin) is predominantly present in the cytosol. G-actin has the potential to polymerize into filamentous actin (F-actin) in vitro and in vivo given the appropriate conditions. Actin filaments are polarized dynamic structures characterized by the presence of the slow growing (-) and fast growing (+) ends. Actin polymerization is initiated by nucleation of a G-actin trimer. This process, along with filament branching, relies on a variety of regulators, among others, the Arp2/3 complex activated by N-WASP, Rho- GTPases and other factors.

The diversity of F-actin structures and associated cellular functions depends not only on polymerization and depolymerization, but on a variety of actin-binding proteins, which can be grouped in G-actin sequestering or associated proteins (e.g. ADF, cofilin, profilin), F-actin capping and severing proteins (e.g. gelsolin, capping protein, severin), actin filament crosslinking and bundling proteins (i.e. fimbrin, α -actinin, filamin), motor proteins (myosins), and membrane anchoring proteins (i.e. ponticulin, talin, vinculin). Most coronins that have been characterized so far belong to the group of actin filament-crosslinking and bundling proteins.

1.1.1. Yeast coronin regulates the actin cytoskeleton by directly interacting with Arp2/3 complex

Crn1p, the only yeast coronin, was independently isolated by two groups using homology cloning and microtubule affinity chromatography, respectively (Goode et al., 1999; Heil-Chapdelaine et al., 1998). The 651-amino-acid protein comprises five WD-repeats, a coiled-coil carboxyl terminus and a central region enriched in proline and charged amino acids. Additionally, it includes a predicted microtubule-binding domain similar to that of the microtubule-binding protein MAP1B. Crn1p was shown to localize to cortical actin patches in a latrunculin A-sensitive manner (Goode et al., 1999; Heil-Chapdelaine et al., 1998), implying that

crn1p localization is dependent on F-actin. Crn1p is an abundant protein indicating a high-affinity binding to F-actin at a 1:1 molar ratio suggesting that the binding appears at the sides of actin filaments (Goode et al., 1999). When added to F-actin in vitro, crn1p bundles the actin filaments. However, if added to actin monomers, yeast coronin instead induces a three-dimensional network formation as shown by electron microscopy and falling ball viscosimetry. Moreover, crn1p accelerates the filament assembly at the barbed end if added to a G-actin solution (Goode et al., 1999). It also binds to microtubules, although considerably weaker than to actin, and can therefore directly crosslink actin filaments with microtubules.

F-actin binding and assembly were mapped to the WD repeats, microtubule binding to the MAP1B homology domain, and actin bundling to the coiled-coil region (Goode et al., 1999). As the coiled coil was shown to participate in dimerization and oligomerization in other coronins (Asano et al., 2001; Spoerl et al., 2002), it may be argued that F-actin bundling depends on crn1p present in the di- or oligomeric state. In vivo, crn1p localization to the cortical actin patches requires both, coiled-coil and actin-binding domains (Humphries et al., 2002). Moreover, crn1p directly associates with the Arp2/3 complex in vitro and in vivo. Crn1p inhibited the actin nucleation activity of the Arp2/3 complex although crn1p alone has a slightly stimulating effect in an actin polymerization assay (Goode et al., 1999; Humphries et al., 2002). The mechanism for the crn1p inhibition of the Arp2/3 complex was explained by a direct interaction between crn1p and the Arp2/3 complex, as was the case in yeast two-hybrid experiments in which the C-terminus of crn1p interacted with Arc35, the subunit responsible for the binding of the Arp2/3 complex to the sides of actin filaments.

The interaction of crn1p and Arp2/3 was considered to regulate the filament branching and thus the formation of complex actin networks important for cell movement and intracellular transport. No pronounced phenotype was reported for the crn1 mutant (Goode et al., 1999; Heil-

Chapdelaine et al., 1998). However, the absence of crn1p appears to enhance the phenotypes of cofilin and actin (ATP-binding pocket) mutants (Goode et al., 1999). Overexpression of crn1p leads to abnormalities in the cytoskeleton organization resulting in swollen cells with actin patches depolarized from the bud region, as well as in the accumulation of spiral or loop actin structures in the cytoplasm (Humphries et al., 2002). These defects were due to the overproduction of crn1p coiled-coil regions, as a truncated form of crn1p lacking the coiled coil does not cause such a phenotype.

1.1.2. Drosophila Dpod1: an actin–tubulin linker regulating the development of the nervous system

Drosophila dpod1 encodes a novel double-core domain 1074-amino acid coronin strongly expressed in the developing nervous system (Rothenberg et al., 2003). In addition to the two core domains, the *Drosophila* protein possesses a predicted microtubule-binding domain similar to that of the microtubule-binding protein MAP1B. In adherent S2 cells derived from mixed *Drosophila* embryonic tissues, Dpod1 co-localizes with both microfilaments and microtubules and is re-localized to microtubules upon the disruption of the actin cytoskeleton. In vitro, Dpod1 crosslinks microtubules as well as microfilaments. Apart from being able to crosslink actin filaments as well as microtubules, Dpod1 is capable of forming bundles containing both microfilaments and microtubules. Co-sedimentation of microtubules with F-actin-coronin bundles has been previously demonstrated in yeast (Goode et al., 1999).

Although Dpod1 is not essential for cytoskeletal organization in S2 cells as shown by the absence of any pronounced phenotype in dpod1 RNAi cells, overexpression of GFP-tagged protein leads to development of highly dynamic neurite-like cell surface projections (Rothenberg et al., 2003). The formation of these projections was further shown to be actin-, but not tubulin-

dependent. Dpod1 acts as an important regulator of neural development in the fly. dpod1 mutant flies are characterized by an aberrant axonal guidance resulting in failures in the target innervation. In particular, axonal fine routing at choice points and turns, but not neurite outgrowth or extension is affected. Overproduction of Dpod1 protein also results in multiple neural phenotypes (Rothenberg et al., 2003). As Dpod1 regulates both microfilament and microtubule architecture, these phenotypes can be explained by aberrant cytoskeleton-related morphogenetic processes in mutant cells, leading to structural abnormalities like axonal breaks, defects in lateral branching and stalling at important decision-making points and thus to defects in target innervation. A model has been proposed linking Dpod1 to scaffolding signalling molecules at the cytoskeleton (Rothenberg et al., 2003), albeit more experimental evidence is necessary to support such a role.

1.1.3. Mammalian short coronin proteins and the actin cytoskeleton

Most of the mammalian coronins belong to the group of actin filament crosslinking and bundling proteins. Coronin 1 is the best-characterized mammalian coronin and is the closest relative of *Dictyostelium discoideum* coronin (Suzuki et al., 1995). It is most strongly expressed in human immune tissues and immune cells and, to a lesser extent, in the lung and brain. On the mRNA level, the skeletal muscle species is larger in size. During the process of murine thymic cell development, peak expression levels of coronin 1 are found in early thymocytes and in adult CD4+CD8- and CD4-CD8+ thymocytes. In thymocytes, the protein localizes to the cytoplasm and to F-actin-rich membrane protrusions especially in stimulated T-cells (Nal et al., 2004). ActA-positive *Listeria monocytogenes*, among other proteins, recruits coronin 1 to their F-actin tails in infected host cells (David et al., 1998).

Two regions that mediate binding to F-actin were determined. One is the N-terminally located KXRHXX-motif conserved in all coronin proteins (Table 1); a second F-actin binding site in coronin 1 was mapped within the domain containing the WD repeats (Oku et al., 2003). A leucine zipper region of the C-terminus mediates homophilic dimerization of coronin 1 (Oku et al., 2005). Human phagocytic leukocytes contain coronin 1 in cytosolic as well as in cytoskeletal fractions. During the course of phagosome formation the peripheral cytoskeletal and cytosolic coronin 1 staining is lost and an association with F-actin around early phagocytic vacuoles can be observed. Dissociation of coronin 1 from the phagosome is accompanied by phosphorylation on serine residues involving PKC. Without the dissociation, the subsequent formation of phagolysosomes is inhibited (Itoh et al., 2002). Recently, coronin 1 has been demonstrated to link the actin cytoskeleton to the plasma membrane in leukocytes (Gatfield et al., 2005). According to the authors, coronin 1 trimerizes using a linker region between the core domain and the C-terminus, while the amino-terminus mediates interaction with plasma membrane (Gatfield et al., 2005). It is unclear whether such coronin 1-mediated interaction between the cytoskeleton and plasma membrane is of biological significance.

Soluble coronin 1 elutes together with phox components in a complex of higher molecular mass from gel filtration, as it binds C-terminally to p40phox, a cytosolic subunit of the NADPH oxidase complex involved in the generation of the microbicidal superoxide burst in neutrophils (Grogan et al., 1997). Furthermore, PKC activation leads to the redistribution of coronin 1 in a phox-protein-dependent manner from the cell cortex to the perinuclear region. A second soluble pool of coronin 1 in human phagocytic leukocytes forms high-molecular-weight complexes independently of the phox proteins. These complexes are solubilized by PI3-kinase activity and may be involved in forming the F-actin structures in early phagosome formation (Didichenko et al., 2000).

In addition, coronin 1 is detected on phagocytic vacuoles of macrophages. Upon internalization of mycobacteria, coronin 1 is transiently recruited to the site of the bacterial entry (Schuller et al., 2001). Moreover, clumps of 10–20 living mycobacteria in phagosomes inhibit the dissociation of coronin 1 and the continued transport of the phagosomes to lysosomes. Retaining coronin 1 on the early phagosome prevents the mycobacterial clumps from lysosomal degradation (Ferrari et al., 1999). Using a dominant-negative approach, Yan and colleagues recently demonstrated that coronin 1 is required for the accumulation of Arp3 on phagosomes, as well as for receptor capping and actin remodeling at forming and early phagosomes (Yan et al., 2005).

Coronin 2 was first described as a phosphoprotein in HCl-secreting gastric parietal cells (rabbit coronin_{se}, (Brown and Chew, 1989; Chew et al., 1997) and is generally found in the gastrointestinal mucosa, but also highly expressed in secretory cells of the kidney and lung, and in smaller amounts in spleen, adrenal and other tissues (Parente et al., 1999). In the kidney coronin 2 primarily localizes to cortical F-actin structures (Parente et al., 1999). The homologous mouse coronin 2 differs from coronin_{se} in a short part of the unique C-terminal region and is ubiquitously expressed and most prominent in the kidney, lung, spleen and liver (de Hostos, 1999; Morrissette et al., 1999; Okumura et al., 1998). On the subcellular level, coronin 2 shows a perinuclear punctate pattern and is localized to early phagosomes (Morrissette et al., 1999). PKC-dependent serine phosphorylation of coronin 2 leads to a partial redistribution of coronin 2 from vesicular structures, which are neither Golgi membranes nor mitochondria, to the leading edge of the induced actin-rich filopodia (Parente et al., 1999). Recently, coronin 2 was shown to co-localize and interact with Arp2/3 complex (Cai et al., 2005). This interaction is mediated by PKC-dependent phosphorylation of serine-2 on coronin 2, and is important for the leading edge dynamics in fibroblasts (Cai et al., 2005).

Coronin 3 is ubiquitously expressed and is most prominent in the brain, lung, intestine and kidney (Hasse et al., 2005; Iizaka et al., 2000; Spoerl et al., 2002). An additional band of higher molecular weight (60 kDa) is detected in the brain and heart, while in the skeletal muscle this band is the only one present. A single RNA species has been described. Coronin 3 is localized to F-actin-rich punctate structures in the cytosol, which are most pronounced around the nucleus and at the cell cortex, especially in lamellipodia and membrane ruffles (Spoerl et al., 2002). Both N and C termini of coronin 3 are required for its cytoskeletal localization and for coronin-3-mediated regulation of cell morphology. The C terminus (aa 315–474) confers membrane association, and removal of its coiled-coil part (aa 444–474) abolishes membrane localization. In vitro, F-actin binding and bundling occurs through the C-terminal fragment preceding the coiled coil (aa 315–444). This fragment interacts with the N terminus and can lead to decreased binding of the C-terminal fragment to F-actin. Conversely, the entire C terminus can recruit the purified N-terminal region to actin filaments probably reflecting the folding pattern of coronin 3 bound to actin. The dissociation constants of both coronin 3 C-terminal fragments binding to F-actin were evaluated at about 8 mM. F-actin binding was saturated at a 1:3 molar ratio for both fragments.

Surprisingly, the C terminus (aa 315–474) forms trimers while the non-coiled-coil C terminus (aa 315–444) forms dimers. The oligomerization is non-ionic and does not require other proteins. Also, endogenous coronin 3 is extracted as trimer from cytosol and membrane fraction (Spoerl et al., 2002). The coiled-coil region of the C terminus contributes to a simultaneous binding of the N-terminal domain and F-actin and to a trimerization of coronin 3, properties which seem to be essential for cellular membrane localization.

Generally, cytosolic, but not particle-associated coronin 3 indicated a high degree of phosphorylation (Spoerl et al., 2002), and coronin 3 can be dephosphorylated in vitro

(A. Rosentreter and C. Clemen, personal communication). PKC activation did not influence the subcellular distribution, but resulted in a decreased level of the coronin 3 protein. This reduction may be due to the 3' UTR of the coronin 3 mRNA containing 14 CUUU repeats similar to the (CUUU)₁₁(U)₈ repeats of MARCKS mRNA (Spoerl et al., 2002). This CUUU₁₄- repeat element is not found in any other mammalian coronin mRNA. In MARCKS mRNA, the element mediates rapid mRNA degradation upon treatment with growth factors or PKC activators (Wein et al., 2003).

1.2. Coronin and POD-1 proteins at the interface of cytoskeleton and trafficking

Intracellular membrane organelles form a highly dynamic continuum intimately connected by means of two major trafficking routes. The membrane flow from the endoplasmic reticulum through the Golgi complex to the cell surface, lysosomes and other organelles is generally described as a biosynthetic pathway. Another trafficking route, the endocytic pathway, connects the plasma membrane with the endosomal system, lysosomes and the Golgi/ER membranes. Subcellular localization and trafficking of the membrane compartments have been shown to rely on the interaction of these structures with cytoskeletal components. Formation of endocytic vesicles at the plasma membrane depends on the interaction of the membrane with cortical actin and several actin-binding proteins including dynamin and cortactin (Cao et al., 2003; Sauvonnet et al., 2005; Yarar et al., 2005). Dynamics of cargo vesicles are mediated by both actin cytoskeleton and microtubules. The interference with any of these systems leads to multiple defects in vesicular trafficking such as an impairment of the formation of the trans-Golgi network and ER export carriers (Waguri et al., 2003; Watson et al., 2005), or of the formation and cytoplasmic progression of the vesicles (Mundy et al., 2002; Yarar et al., 2005). Several

studies hinted at a possible function of coronin proteins at the interface of the cytoskeleton and intracellular membrane transport.

1.2.1. Drosophila coro possibly acts as a linker between the actin cytoskeleton and membrane transport

Recently, a novel conventional coronin gene has been identified in *Drosophila* (Bharathi et al., 2004). *coro* encodes a predicted 528-amino-acid protein harboring a core domain and a C-terminal coiled-coil region. The *coro* gene is ubiquitously expressed at high levels in all cell types with the exception of the larval CNS. Mutations in the gene are lethal at early to late pupal stages and exhibit a number of appendage phenotypes including shortened, ventralized, thick legs, defective wing margins and malformed eyes with improper ommatidial organization. On the cellular level, *coro* mutations result in a disruption of the cytoskeleton in the wing imaginal discs. Actin filaments appear retracted and the cortical actin reduced, leading to abnormal cell morphology (Bharathi et al., 2004).

Importantly, it has been suggested that the *coro* gene genetically interacts with the *syx1A* gene encoding a *Drosophila* SNARE protein participating in secretion and calcium channel functions (Schulze et al., 1995; Wu et al., 1999). The *coro* mutant phenotype is similar to that of *syx1A*. Furthermore, overexpression of *syx1A* on a background of *coro* mutation by imprecise P-element excision enhances lethality and also causes enhancement of the *coro* phenotype implying an interaction of the syntaxin 1A and coronin genes (Bharathi et al., 2004). In *coro* mutants, the GFP-fused morphogen Dpp accumulates in endocytic vesicles docked at the inner side of the plasma membrane. Further, Dpp degradation is slowed down, resulting in uniform Dpp presence along the anteroposterior wing disc axis and in disc overgrowth (Bharathi et al., 2004).

Drosophila coro thus participates in establishment of the Dpp morphogen gradient by regulating the intracellular routing of Dpp.

It may well be that the defect in the cortical actin structures reported for *coro* mutants (Bharathi et al., 2004) causes abnormal subplasmalemmal vesicle transport resulting in accumulation of Dpp-containing vesicles. Such an accumulation by interfering with actin structures was also demonstrated in cytochalasin-D-treated acinar epithelial cells (Da Costa et al., 2003) and in the case of loading actin filaments with N-ethylmaleimide-treated myosin S1 in lamprey reticulospinal synapses (Shupliakov et al., 2002).

1.2.2. C. elegans POD-1, an actin-binding protein participating in vesicular trafficking

A POD-1 protein was first purified in a screen designed to isolate *C. elegans* actin-binding proteins (first named CABP11) (Aroian et al., 1997). In early worm embryos, the protein co-localizes with actin in the cortical region and, in addition, exhibits a punctate cytoplasmic staining pattern. Loss of *pod-1* gene activity results in defects in anteroposterior polarity in early embryos in that the second AB and P1 cell division occurs synchronously and in parallel orientations, instead of the wild-type pattern, which is characterized by the P1 cell dividing after AB and having a division plane perpendicular to that of AB (Rappleye et al., 1999). Furthermore, mutant embryos do not separate polar bodies. Additional defects appear in vesicular trafficking processes. Firstly, the polar granules are found throughout the cytoplasm of mutant embryos, whereas normal embryos transport the polar granules towards the posterior pole. Secondly, mutant cells accumulate abnormally large intracellular membrane structures as shown by staining with an antibody recognizing plasma membrane and vesicles of endocytic origin. Finally, a defect in the inner eggshell layer formation also indicates abnormal exocytic functions. This defect has

been illustrated by an increased dye permeability and osmotic sensitivity of the eggshell (Rappleye et al., 1999).

C. elegans POD-1 co-localizes with cortical actin and cytoplasmic structures and facilitates trafficking processes. The function of POD-1 may be to regulate the attachment of vesicular structures to the actin microfilaments and thus facilitating oriented trafficking. The accumulation of abnormal cytosolic membrane structures in pod-1 mutants can be explained by the absence of such vesicle-microfilament binding. Based on the information available on yeast crn1p (see above), it might be reasonable to speculate that such binding is Arp2/3-dependent. However, the absence of the coiled-coil domain required for Arp2/3 regulation in the yeast protein makes this less likely (Humphries et al., 2002). The eggshell phenotype can be explained by the lack of proper interaction of exocytic vesicles with the cortical actin cytoskeleton or by abnormal intracellular trafficking of such vesicles resulting in misdirection of the Golgi–plasma membrane flow.

1.3. Mammalian coronins with unexplored functions

To date, seven mammalian genes with several transcriptional products have been identified (Table 1). Except for isoform C of coronin 6 lacking the fourth WD-repeat domain, all short coronins contain five predicted central WD repeats. Functional data or biochemical properties are not available for coronins 4, 5 and 6. Coronin 4 is restricted to colon, prostate and testis, but also described in brain tissue (Nakamura et al., 1999; Okumura et al., 1998; Zaphiropoulos and Toftgard, 1996). Coronin 5 is also present in neuronal tissue and to a lesser degree in heart and ovary (Nakamura et al., 1999). Coronin 6 (accession number NP_624354-6) was detected in the brain.

1.4. Clinical implications

Recent data suggest that coronin proteins participate in such processes as an antimicrobial defense and neuronal development and function. Coronin 1 has been shown to participate actively in the innate defense reactions on the cellular level (Gatfield et al., 2005; Itoh et al., 2002). The functional connection between the actin cytoskeleton, coronin 1 protein and phagocytosis of pathogenic mycobacteria has already been discussed above. Clinical investigations have revealed that coronin 1 and the Arp2/3 complex 20 kDa subunit are downregulated in the fetal Down syndrome brain cortex (Weitzdoerfer et al., 2004). Both are proteins apparently involved in the dysgenesis of the brain and the associated mental disabilities. In murine brain all areas express coronin 3 during embryogenesis and the first postnatal stages (Hasse et al., 2005). Postnatally, the expression in the gray matter decreases, except for hippocampal and cerebellar Purkinje neurons, while levels in the white matter increase in the course of myelination (Hasse et al., 2005).

Cultured neuro-2a and PC-12 cells transfected with various GFP-tagged coronin 3 versions favor a role for coronin 3 in neuronal function, morphogenesis and possibly migration. Truncated proteins efficiently suppress neurite formation and either stimulate or inhibit noradrenaline (norepinephrine) secretion of PC-12 cells (A. Hasse and C. Clemen, personal communication). Coronin 5 accumulates at neurite growth cones and co-localizes with focal adhesions as well as with stress fibers. It co-precipitates with vinculin, a major component of focal contacts and also binds directly to F-actin in vitro (Nakamura et al., 1995). Coronins 3 and 5 may be involved in neuronal migration, neurite extension and synapse formation by means of rearranging F-actin and linking it to the plasma membrane.

Coronin 1 is abundantly expressed in T- and B-lymphocytes and macrophages (Didichenko et al., 2000; Goode et al., 1999; Itoh et al., 2002; Okumura et al., 1998; Schuller et al., 2001). Apart from an expression in thymic cells, coronin 1 was shown to be involved in processes of membrane organization of nascent phagosomes and associated with their F-actin coat. Later, a dissociation of coronin 1 seems to be necessary for further phagosome processing. Clumps of phagocytosed mycobacteria cause the retention of coronin 1 on the early phagosome and inhibit their delivery to lysosomal degradation (Ferrari et al., 1999). The recruitment of coronin 1 to the phagosome may be regulated endogenously by PKC and PI3-kinase activity, and exogenously by factors like that of living mycobacteria. Soluble coronin 1 is involved in generating focal microbicidal superoxide bursts. These data strongly suggest an important contribution of coronin 1 to innate defense reactions.

Coronin proteins play important roles in development and disease: In *Drosophila* and *C. elegans*, coronin and POD-1 mutants exhibit a number of developmental defects ranging from abnormal determination of cell polarity and formation of morphogenetic gradients to aberrant axonal guidance and target innervation (Bharathi et al., 2004; Rappleye et al., 1999; Rothenberg et al., 2003). Several mammalian coronins are strongly expressed in the CNS and possibly involved in the development of the nervous system. Coronin 3 demonstrates a highly dynamic expression pattern in the embryonic brain implying that differential activity of this protein may participate in the regulation of brain development, probably together with other coronins expressed in the developing brain (Hasse et al., 2005). Although some coronins have been studied in detail, biochemical and functional properties of their majority is unclear. Future experiments need to be directed at functional properties of coronin proteins. There are still significant gaps in our understanding of the regulation of coronin genes and proteins, too. The positions of coronin proteins in the complex protein interaction networks have not yet been characterized. Functions

of the central core domain particularly require further investigation. Clearly, based on the well-established functions in the regulation of the actin cytoskeleton and membrane trafficking as well as being implicated in many developmental processes and in disease, this protein family deserves further investigation.

2. AIMS OF THE WORK

Recently, a novel mammalian coronin family member was identified and designated coronin 7 (A. Schulze, diploma thesis, Cologne University, 2001). My primary aims were:

- To analyze the cellular localization and dynamics of coronin 7 (Crn7) using biochemical methods, immunofluorescence and electron microscopy;
- To characterize Crn7 interaction partners;

To reveal the function of Crn7 in mammalian cells using gene interference (RNAi).

3. RESULTS

Crn7 is a ubiquitous mammalian coronin family member. The protein is distributed between the cytosol and Golgi, where it is present at the outer side of the membrane. Golgi localization of Crn7 depends on tyrosine phosphorylation and the integrity of ER-to-Golgi transport. The protein intimately associates with the Golgi membrane and does not require coatomer for its localization. Crn7 is an essential protein, as its knockdown by RNAi leads to a dramatic time- and concentration-dependent decrease in cell viability. Crn7 RNAi cells display scattered Golgi morphology, as demonstrated by electron and light microscopy. Most importantly, the knockdown leads to the block of protein export from the Golgi complex, while the import into the organelle, both anterograde and retrograde, remains unaffected. Further, I established that Crn7 interacts with AP-1 adaptor protein complex participating in the Golgi export by linking cargoes to the clathrin coat.

3.1. Crn7 sequence analysis.

3.1.1. Crn7 is a mammalian long coronin and POD-1 homologue.

A complete cDNA for human a novel human WD-repeat protein has been previously cloned by reverse transcription PCR from a HEPG2 cDNA clone HEP08253 (accession number AK025674, obtained from the MRC Centre, Cambridge, UK) using information from the EST database (A. Schulze, Diploma thesis, University of Cologne, 2001). The obtained sequence contains a single open reading frame encoding a 925-amino acid protein (Fig. 2) with a predicted molecular weight of 100.5 kDa and a predicted isoelectric point of 5.6. The protein is characterized by the presence of six to ten WD repeats depending on the prediction algorithm. The WD repeats are clustered in two groups. Sequence alignment (see A. Schulze, Diploma thesis, University of Cologne, 2001) allowed us to postulate that the protein belongs to the

coronin family, and to name it coronin 7 (Crn7). As all coronins, Crn7 possesses a characteristic ...SKFRH... motif upstream of both WD repeat clusters.

```

1      mnrfrvskfr htearprrre swisdiragt apscrnhiks scsliafn sd rpgvlgivpl
61     qgqgedkrrv ahlgchsd lv tdl dfspfdd fllatgsadr tvklwrlpgp gqalpsapgv
121    vlgpedlpve vlqfhptsdg ilvsaa gttv kwdaakqpp ltelaahgd l vqsavwsrdg
181    alvgtackdk qlrifdprtk prasqstqah ensrdsrlaw mgtwehlvst gfnqmrerev
241    klwdtrffss alasltdts lgclvp ll dp ds gl l vlagk gerqlycyev vpqqpal spv
301    tqcvlesv lr gaalvprqal avmscev lr v lqls dta ivp igyh vprkav efhedlf pdt
361    agcvpatdph swwagdnq qkv slnpacr phpsft s clv ppa eplpdta qpavmet pvg
421    dadaseg fss ppss ltpst psslqps l ss tsqig tps l rslq sllq ps skfrh aqgtv
481    lhrdsh itnl kglnl ttpge sdgfcanklr vavpl l ssgg qvavle l rkp grlp dtal pt
541    lqngaa vtdl awdpfdphrl avagedarir lwrvpaegle evl ttpetvl tghtekic sl
601    rfhp laanvl assy dl tvr iwdlqagadr lklqghqdqi fslaw spdgq qlatv ckdgr
661    vr vyrprsgp eplqeg pgpk g g rgariv wv cdgr cl l vsg fd sqserq l lyeaealagg
721    plavlgldva p st l l p sdy dp dtgl vltgk gd trvfl yel 1 pes pfflec nsft spdp h
781    glvllpk tec dv revelmrc lrlrq sslep vafrlp rvrk effqddvfpd tavi wepv ls
841    aeawlq gang qpwlls lqpp dm spv s qap r eap arrap ss aqyleeks dq qk keell nam
901    vaklgn redp lpqdsf egvd edewd

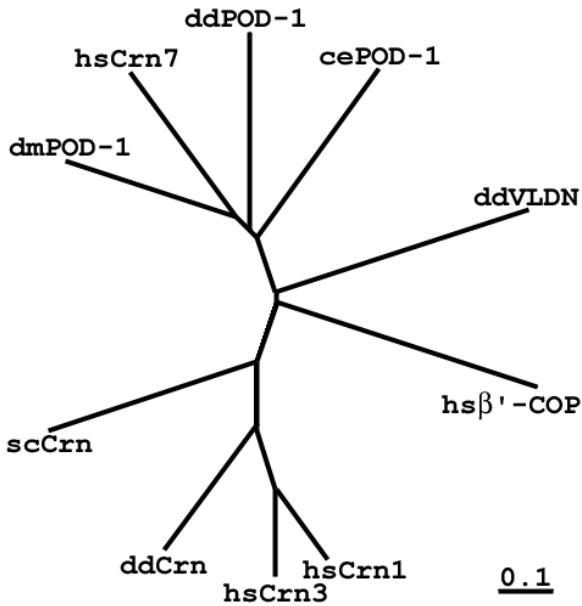
```

Fig. 2. Predicted amino acid sequence of human Crn7 protein. Core domains containing WD repeats are shown in blue, coronin signature motifs (Rybakin and Clemen, 2005) are highlighted in black, a serine, proline and threonine-enriched sequence is underlined. YxxΦ motifs are highlighted in yellow.

The predicted WD repeats of Crn7 are grouped in characteristic two coronin core domains, as in *C. elegans* POD-1 and dPOD-1 from *Drosophila*. Crn7 protein is 46% and 47% homologous and 30% and 29% identical to Dpod-1 and POD-1, respectively as predicted by NCBI BLAST server using BLOSUM62 matrix. Similarly to the worm and fly homologues, Crn7 lacks the C-terminal coiled-coil region. Phylogenetic analysis using cluster algorithm clearly positions Crn7 and both previously described POD-1 proteins in a group distinct from other coronins (Fig. 3).

A structural peculiarity of Crn7 is the presence of a 47-amino acid long proline, serine and threonine-enriched stretch upstream of the second group of WD repeats designated a PST

motif (Fig. 2). Such sequence is not found in any other coronin proteins, and its function (if any) remains unclear.



*Fig. 3. Phylogenetic analysis of the coronin family members, including POD-1 proteins, performed using the cluster algorithm. dmPOD-1 – Drosophila dPOD-1 protein, cePOD1 – C. elegans POD-1, ddPOD-1 – POD-1 protein from Dictyostelium discoideum, hsCrn1, 3, 7 – human coronins 1, 3 and 7, respectively, ddCrn – Dictyostelium coronin, scCrn – yeast (*Saccharomyces cerevisiae*) coronin, ddVLDN – Dictyostelium villidin, hsβ'-COP – human β'-COP. Multiple WD-repeat proteins villidin and β'-COP are clearly forming outgroups with regard to both coronins and POD-1 proteins. The bar corresponds to 10% of amino acid substitution within the branch.*

Additionally, Crn7 harbours two putative copies of a classical tyrosine-based sorting signal downstream of each core domain (Fig.1). This feature is also unique for Crn7, and will be discussed later.

3.2. Tissue distribution and developmental dynamics of Crn7

Using a monoclonal antibody K37-142-1 raised against the C-terminus of Crn7 (Rybakin et al., 2004), we analyzed the distribution of the protein in murine tissues by western blot. Crn7 was found to be ubiquitously expressed in all studied tissues, except for the heart and skeletal muscle (Fig. 4). These findings are in good agreement with Northern blot data shown previously (A. Schulze, Diploma thesis, University of Cologne, 2001). K37-142-1 mAb is used in all further experiments to visualize Crn7.

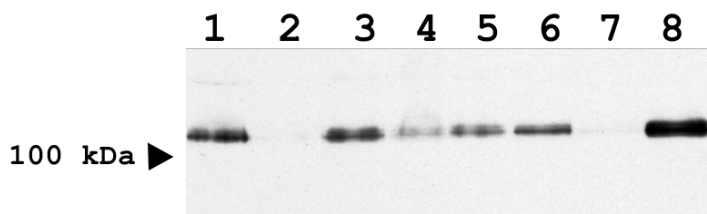


Fig. 4. Tissue distribution of the Crn7 mRNA and protein. Top panel, tissue lysates were separated on 10% SDS-polyacrylamide gels, blotted onto a nitrocellulose filter and probed with monoclonal anti-Crn7 antibody. 1 - brain, 2 - heart, 3 - liver, 4 - lung, 5 - kidney, 6 - testis, 7 - muscle, 8 - thymus. Anti- β -actin monoclonal antibody was used to confirm equal loading (not shown).

Using indirect immunofluorescence, we studied the expression pattern of the Crn7 protein in the mouse. The strongest expression is found in the early postembryonic brain, thymus, intestine, skin and in the eye (Fig. 5). In the brain cortex, the Crn7 protein is restricted to the most apical cell layers before postembryonic day 10 and shifted to a population of more basal cells thereafter, whereas in the hypothalamus the protein is detected in the same set of profound big neurons throughout development. In addition, the protein is found in the bodies and dendrites of

Purkinje cells in the cerebellum. In the skin, Crn7 is only present in the apical epidermis layers (Fig. 5). The differentiating cells in the embryonic eye are also found to be Crn7 positive. Here, Crn7 is found in developing lens fibers. In adult mice, the protein is strongly expressed in the outer plexiform layer of the retina, where the rods are located (data not shown). Interestingly, in the intestine, the protein is found not only in terminally differentiated epithelial cells, but also in the crypt epithelium were the stem cells are located (Fig. 5J).

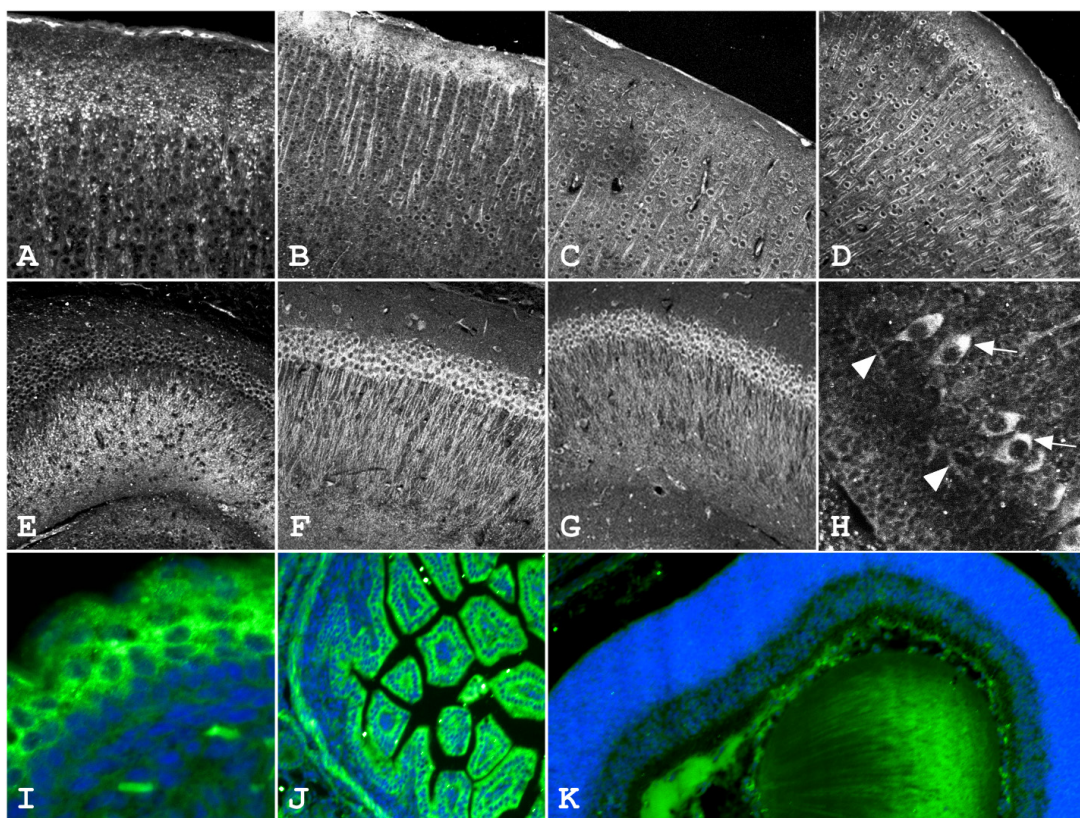


Fig. 5. Immunolocalization of the Crn7 protein in paraformaldehyde-fixed murine early postembryonic tissues. A-D, sections through the brain cortex at the postembryonic days 5, 10, 20 and 30, respectively. E-G, section through the hippocampus at the postembryonic days 10, 20 and 30, respectively. H, localization of the Crn7 protein in the Purkinje cell bodies (arrows) and dendrites (arrowheads). I-K, embryonic skin, intestine and lens, respectively, at the day 16 of development. Top of the images A-G and

I correspond to the apical side of the corresponding organs. Immunostaining was performed using monoclonal anti-Crn7 antibody (green in I-K). Sections were counter-stained with DAPI (blue in I-K).

3.3. Subcellular localization of Crn7

3.3.1. Crn7 is present in the cis-Golgi and in the cytosol

Using indirect immunofluorescence, we analyzed the cellular distribution of Crn7. The protein was found in vesicle-like structures and in a Golgi-like perinuclear compartment (Fig. 6). The characteristic Crn7-positive perinuclear structure was prominent in NIH 3T3 fibroblasts, HeLa, Vero and other cell types. Crn7 protein co-localizes with cis-Golgi markers β -COP and Erd2p in the Golgi region as shown by indirect immunofluorescence (Fig. 6). It is noteworthy that (a) in both cases the Crn7 antibody stains a broader region than both Golgi marker antibodies (Fig. 6C, F, arrows), and (b) the cytosolic Crn7-positive vesicles are clearly distinct from the Erd2p- or β -COP-positive ones (not shown). Cis-Golgi localization of Crn7 was further confirmed by immunostaining NIH 3T3 fibroblasts expressing GFP-fused cis-Golgi markers p23 and GM130 with Crn7 antibody (data not shown). Importantly, although we were able to observe a certain co-localization of Crn7 with the trans-Golgi marker TGN38, such co-localization was restricted to the proximal Golgi region and almost absent in the trans-most cisternae (Fig. 6I).

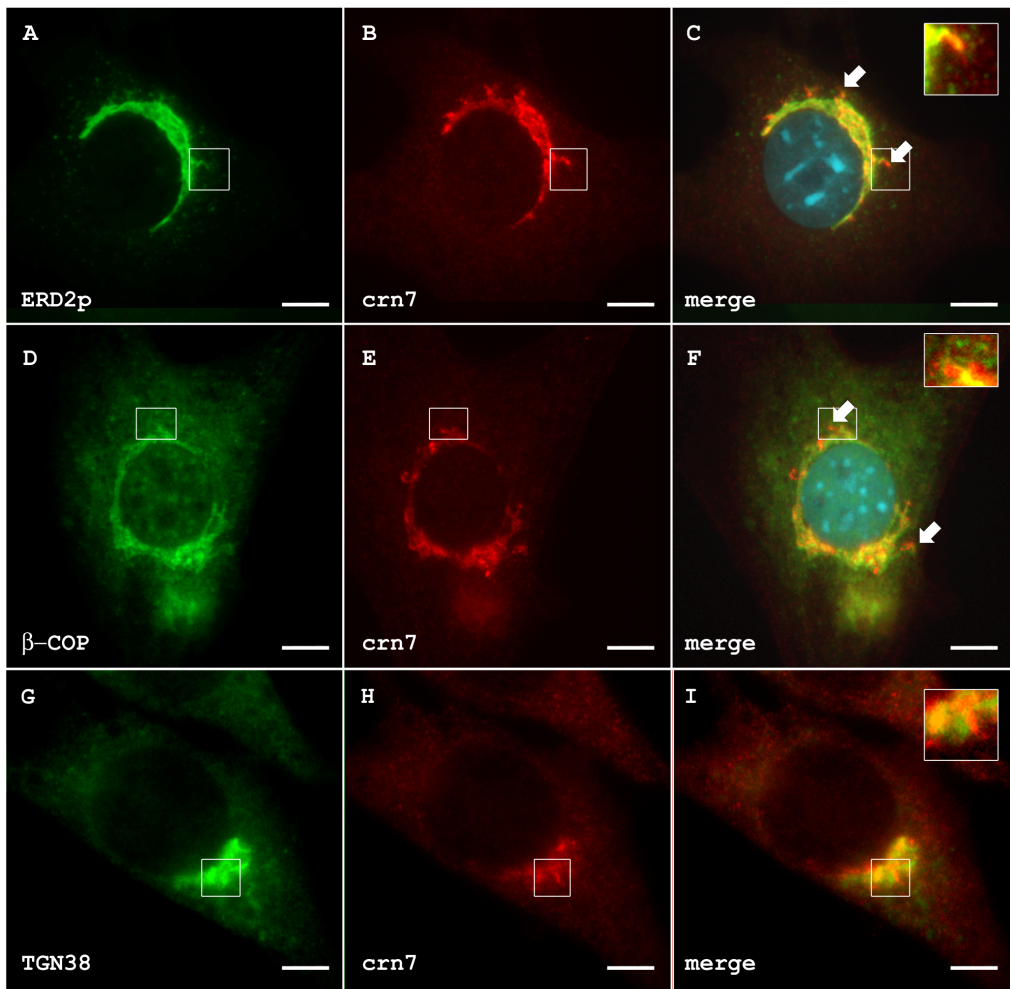


Fig. 6. Immunolocalization of the Crn7 protein in NIH 3T3 cells. Paraformaldehyde-fixed cells were stained with monoclonal anti-Crn7 antibody (B, E, H) and rabbit polyclonal antibodies against either Erd2p (A), β -COP (D), or TGN38 (G). Primary antibodies were detected with goat anti-mouse antibody conjugated with Cy3 (red) and sheep anti-rabbit antibody conjugated with FITC (green). C, F, I, merged false color images. Insets in C, F, I correspond to the areas marked in A-C, D-F and G-I, respectively. Bar, 10 μ m.

Using differential centrifugation, we established that only a minor pool of Crn7 is localized to intracellular membranes. The protein is unequally distributed between the cytosol and membrane fractions, the bulk of it being found in the cytosol (Fig. 7A), where it is present in a free state (200,000g supernatant) as well as in large protein complexes (200,000g pellet). The

membrane-associated Crn7 protein can be extracted from the 10,000g fraction upon treatment with Triton X-100 (Fig. 7B). As a control, we used anti- β -actin antibody (Fig. 7B, lower panel), showing that only the detergent-sensitive membrane components have been extracted, but not cytoskeletal elements.

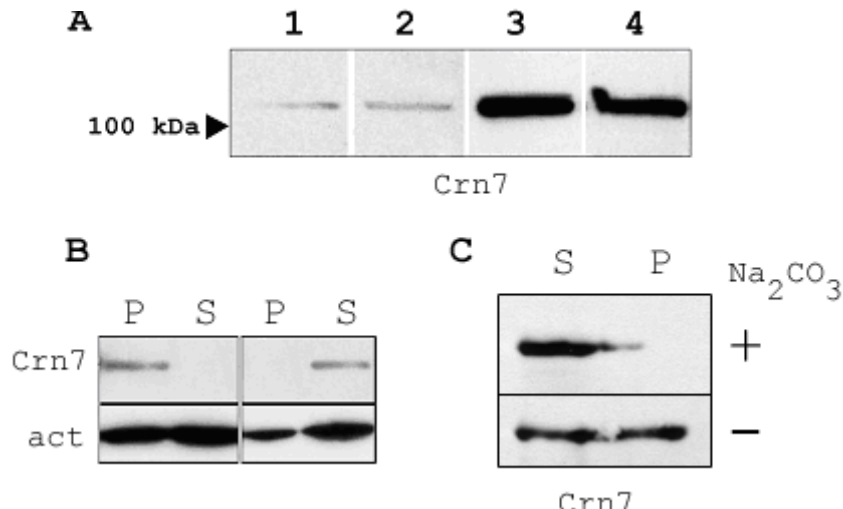


Fig. 7. Crn7 is present on Triton-soluble membranes. A, differential centrifugation experiment showing the presence of the Crn7 protein in heavy membrane / cytoskeletal fraction (10,000g pellet, lane 1), light membrane fraction (100,000g pellet, lane 2), cytosolic protein complexes (200,000g pellet, lane 3) and cytosol (200,000g supernatant, lane 4). B, solubilization of membrane compartments from the 10,000g pellet with Triton X-100. The 10,000g pellet was resuspended in homogenization buffer (Spoerl et al., 2002) and separated into two aliquots. One aliquot was treated with 0.5% Triton X-100 for 30 min at 4°C, the other served as control. Both aliquots were centrifuged again and pellets and supernatants analyzed by western blot. P - 10,000g pellet, S – supernatant. Left, control pellet; right, Triton X-100-treated pellet. Top panels, western blot with anti-Crn7 antibody, bottom panels, with anti- β -actin antibody. C, Crn7 is extracted from membrane fraction by incubation with sodium carbonate (see 3.3.2). Upper panel, sodium carbonate was added to PNS of HeLa cells for 30 min on ice to make 100 mM. PNS was then centrifuged at 100,000g to separate membranes from cytosol. Lower panel, PNS was incubated with equal volume of PBS and fractionated as above.

To localize the protein more precisely within the Golgi complex, we used confocal microscopy to study its co-localization with cis- and the trans-Golgi markers in HeLa cells treated with nocodazole, which is known to partially disrupt Golgi stacks leading to the formation of ministacks where the positions of cis- and the trans-Golgi proteins can be microscopically distinguished (Neubrand et al., 2005). Upon application of 20 $\mu\text{g ml}^{-1}$ nocodazole for 2 hrs, Crn7 co-localized with a fraction of the cis-Golgi compartments positive for GM130 (Fig. 8A-C), but not with TGN38-positive trans-Golgi-derived compartments (Fig. 8D-F). Thus, Crn7 labels a subcompartment of the cis-Golgi.

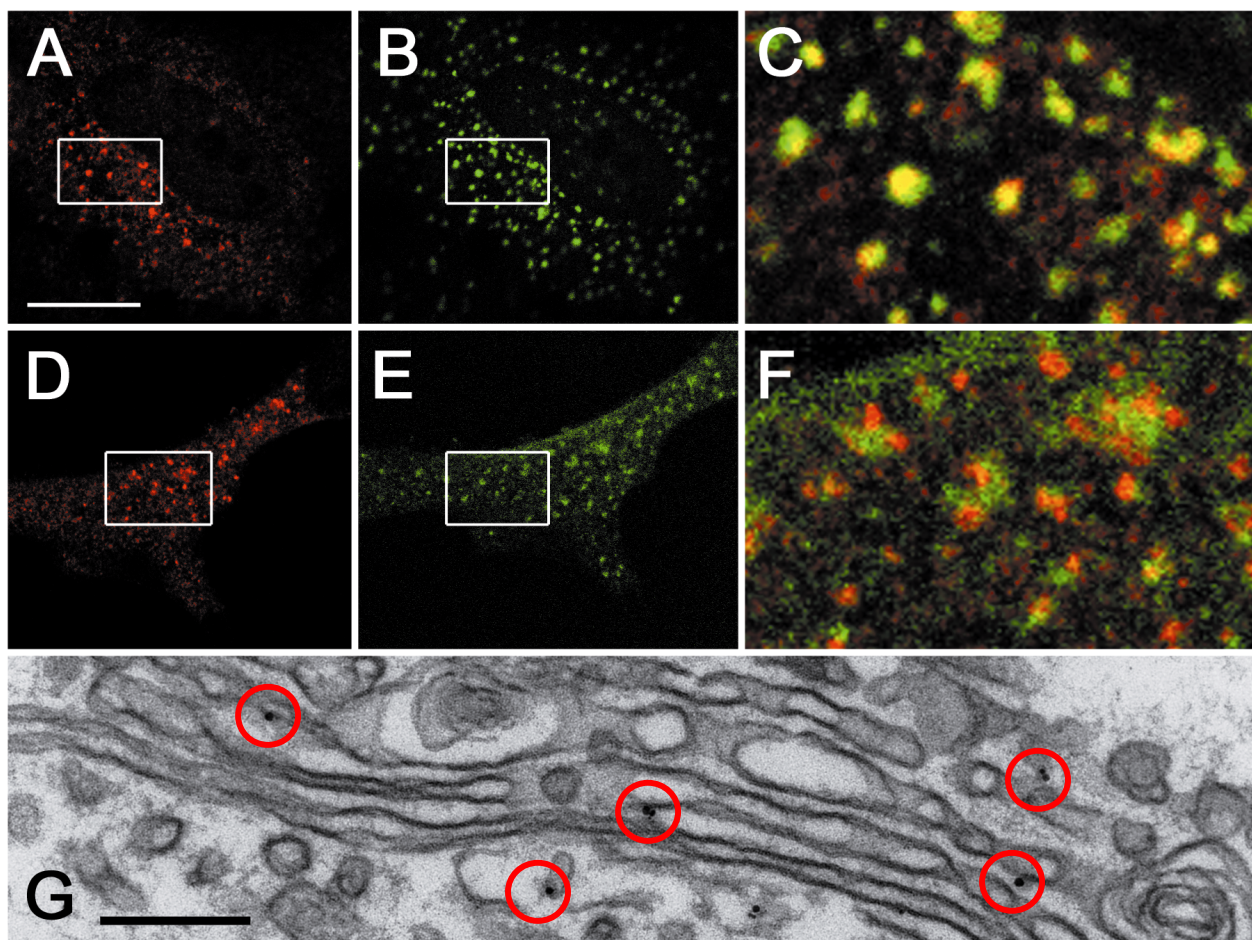


Fig. 8. Crn7 is localized to the outer side of the cis-Golgi membranes. A – F, HeLa cells were treated with nocodazole at 20 $\mu\text{g ml}^{-1}$ for 2 hrs, fixed and stained for Crn7 (A, D), GM130 (B) or TGN38 (E). C, F – merged images corresponding to areas highlighted in A, B and D, E. Size bar, 10 μm . G, Electron

micrograph demonstrating Crn7 immunostaining (red circles) at the outer side of Golgi membranes in HeLa cells. Size bar, 200 nm.

The cytoplasmic Crn7-labelled structures (see Fig. 7) do not correspond to the intermediates of the endocytic pathway, as they do not co-localize with transferrin-positive compartments after 1, 5, 10, 30 or 60 minutes of the internalization of FITC-labelled transferrin in Triton-permeabilized cells (Fig. 9 and not shown) and do not show any Rab5 or LIMP-1 staining (data not shown). We assume that these structures represent large protein complexes constituting the cytosolic pool of the Crn7 protein.

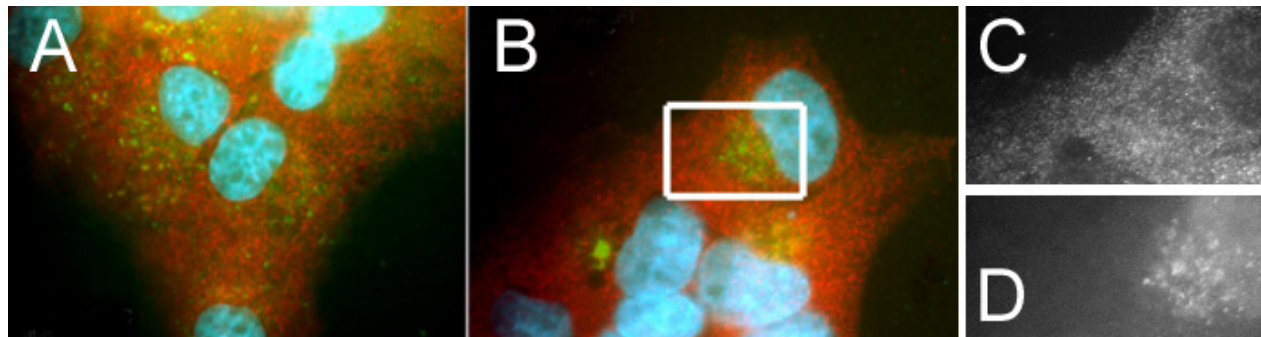


Fig. 9. Crn7 is not present in early and late endosomal compartments positive for transferrin. HeLa cells were allowed to internalize Tf-FITC for 10 (A) or 30 (B-D) min on ice, then fixed and stained for Crn7 (red). C, D, - areas highlighted in B. C - Crn7 antibody staining, D, Tf-FITC signal. Note the exclusion of Crn7 from the late endosome/lysosome accumulation zone (C, D). Golgi Crn7 staining is absent due to permeabilization with Triton X100.

3.3.2. Crn7 is localized to the outer side of Golgi membranes

Further, we exploited the topology of Crn7 - Golgi membrane interactions. We hypothesized that the protein is present at the outer side of Golgi membranes, as it does not

possess predicted signal sequences, signal cleavage or transmembrane sites (as predicted by PSORTII algorithm, (Nakai and Horton, 1999). To prove this hypothesis, we first used the Crn7 antibody and 5-nm immunogold detection to visualize the protein in rat Purkinje cells. Crn7 could be found only at the outer side of Golgi membranes, but not at the inner side or in the lumen (Fig. 8G). The conclusion that Crn7 is localized to the cytosolic side of the Golgi membrane was additionally confirmed by carbonate extraction (Fig. 7C) and proteinase K protection experiments, where Crn7 could not be protected by membranes from proteinase added to membrane fraction (not shown).

3.3.3. Stable association of Crn7 with the Golgi requires the integrity of ER-to-Golgi transport

Brefeldin A (BFA) causes the GTP-to-GDP exchange on Arf1 GTPase and rapid dissociation of Arf1 (Fig. 10) and COPI coat from the membranes (Peyroche et al., 1999). Following this, Golgi membranes start fusing with the ER, and resident Golgi proteins are gradually redistributed to the ER (Lippincott-Schwartz et al., 1989). We treated cells with brefeldin A and assayed β COP and Crn7 dynamics (Fig. 11A-F). Already after one minute of BFA treatment, no typical β COP Golgi staining could be observed by immunofluorescence (Fig. 11E), well in agreement with published data on Arf1 dynamics (Presley et al., 2002).

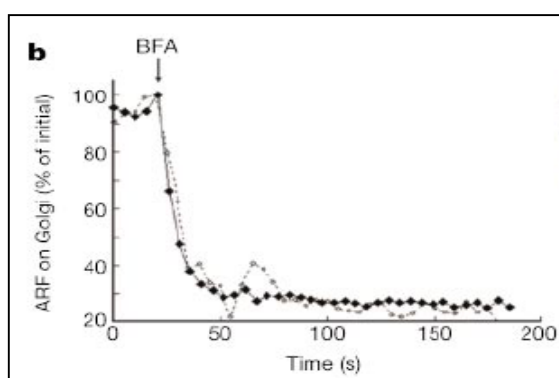


Fig. 10. Effect of Brefeldin A (BFA) on the presence of small GTPase Arf1 on Golgi membranes (from Presley et al., 2002).

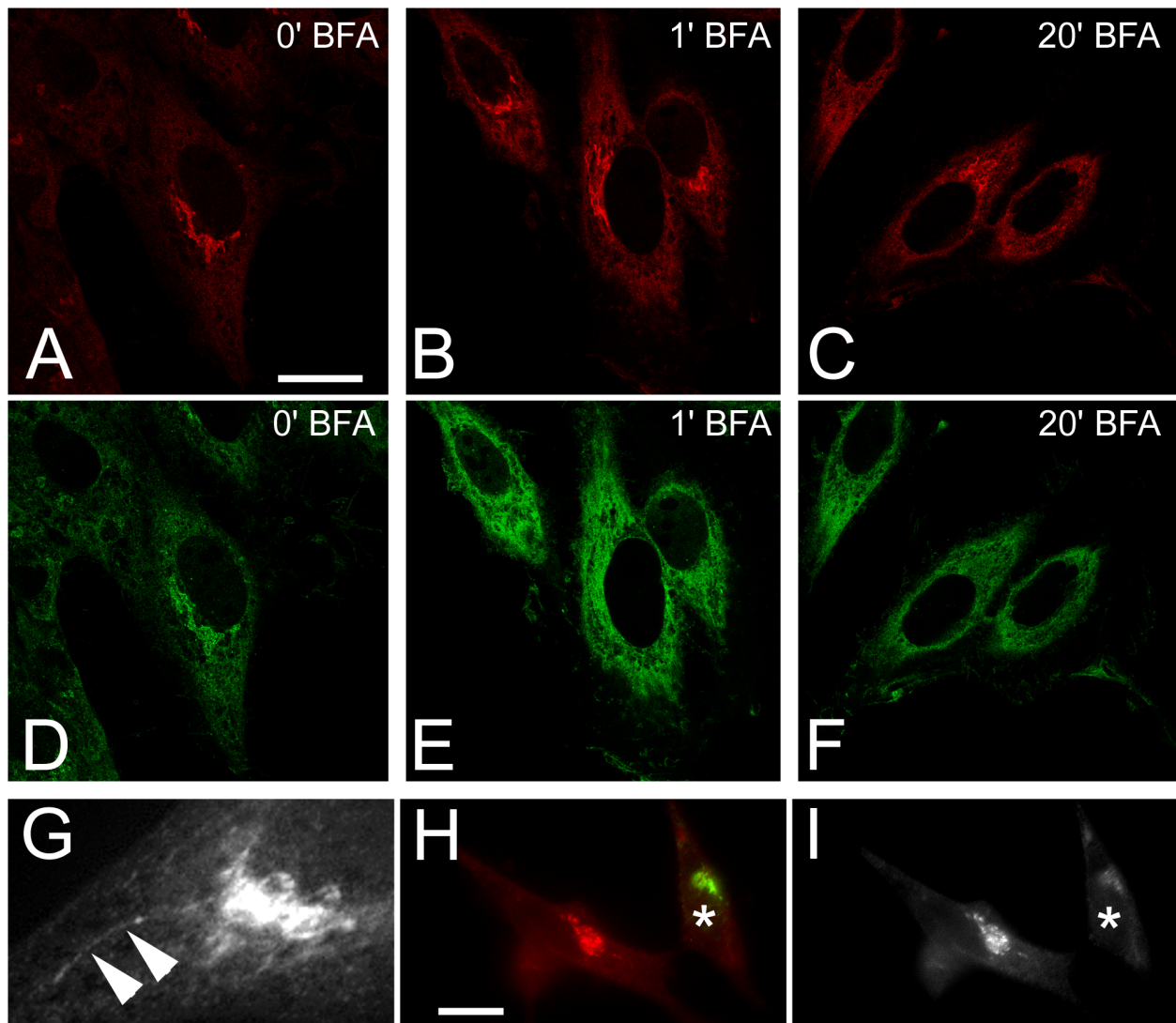


Fig. 11. Crn7 is a structural Golgi protein, and depends on ER-to-Golgi transport in its localization. A – F, HeLa cells were treated with 5 $\mu\text{g ml}^{-1}$ brefeldin A for 1 min (B, E) or 20 min (C, F), fixed and stained for Crn7 (A-C) or β COP (D-F). Size bar, 20 μm . G, Fixed HeLa cell demonstrating the presence of Crn7 on an ER-Golgi intermediate (arrowheads) formed upon the application of BFA for 15 min. H, I, HeLa cells overexpressing GFP-Syn5 (asterisks) are characterized by reduced presence of Crn7 at Golgi membranes. H, Merged image, red, Crn7, green, GFP-Syn5. I, Crn7. Size bar, 20 μm .

Although Crn7 Golgi staining was gradually reducing upon application of BFA, β COP dissociation did not result in the same rate of dissociation of Crn7, and some protein was present

on the collapsing Golgi even 20 min after the beginning of treatment (Fig. 11C). Such dynamics of Crn7 dissociation upon the application of BFA suggest that Crn7 is a structural protein intimately connected to the Golgi membrane. Interestingly, Crn7 was present at chimaeric tubular intermediates apparently connecting Golgi remnants with the ER (Fig. 11G). This finding additionally confirms the presence of Crn7 on Golgi membranes, rather than in the Golgi matrix.

Next, we tested whether Crn7 localization on Golgi membranes depends on the integrity of the ER-to-Golgi trafficking system. Recently, a *cis*-Golgi t-SNAREs complex was shown to participate in the late stages of ER-to-Golgi transport (Zhang and Hong, 2001). The complex consists of four SNARE proteins, syntaxin 5 (Syn5), GS28, Bet1 and Ykt6. Syntaxin 5 was previously shown to specify docking sites for both COPI and COPII vesicles in the Golgi complex (Hui et al., 1997, and references therein). In particular, Syn5 inhibits the import of the vesicular stomatitis virus G-glycoprotein (VSVG) into the Golgi complex if overexpressed, leading to accumulation of cargo in pre-Golgi intermediates (Dascher et al., 1994). We overexpressed GFP-Syn5 in HeLa cells and examined Crn7 localization by immunostaining. The cells expressing GFP-Syn5 exhibit a substantial increase in cytosolic Crn7 staining, and reduced amount of Crn7 on Golgi membranes (Fig. 11H,I). Thus, Crn7 requires the intact influx of certain ER-derived material to be localized to the Golgi.

Because Crn7 lacks any signal peptide and is present in both cytosol and Golgi (see above), we imply that it is recruited to the outer side of Golgi membrane from the cytosol rather than to the Golgi lumen or inner membrane side from the ER. This implication is confirmed by our studies on Crn7 topology using biochemical methods and electron microscopy. Thus, the observed inhibitory effect of Syn5 overexpression on the Golgi localization of Crn7 can hardly be due to the direct block of its import from the ER. It is intriguing to speculate that the Golgi localization of Crn7 is driven by another protein imported from the ER in a Syn5-dependent

manner. Interaction of Crn7 with this unidentified partner might be dependent on its tyrosine phosphorylation, as the membrane-associated Crn7 is phosphorylated on tyrosine residues, while the cytosolic protein is not (see above).

3.3.4. Properties of cytosolic and membrane-associated forms of Crn7

We analyzed the Crn7 protein in membrane and cytosolic fractions by means of 2D gel electrophoresis. Our results evidence that the pI values of the cytosolic form of the protein range between 5.2 and 6.0 with a peak corresponding to the predicted value of 5.6, whereas the membrane-associated form has pI values ranging from 4.5 to 6.0 (Fig. 12A), inferring that the membrane bound form is phosphorylated. Furthermore, when we immunoprecipitated Crn7 from the cytosol and membrane fractions (10,000g pellet) using Crn7 antibody coupled to protein G-sepharose beads in the presence of phosphatase inhibitors the precipitated protein specifically reacted with an anti-tyrosine antibody. No labeling was observed with phosphoserine / threonine specific antibodies (data not shown). Moreover, our results indeed confirm that it is the membrane-associated, but not cytosolic form of Crn7, which is phosphorylated on tyrosine residue(s) (Fig. 12B). Importantly, tyrosine phosphorylation does not only correlate with Crn7 presence in the membrane pellet, but also is required for it. We incubated HeLa cells in the presence of tyrosine kinase inhibitor genistein (1 hr, 100 µg/ml, 37°C), prepared PNS and subfractionated it by centrifugation at 100,000g. Fig. 12C demonstrates that inhibition of tyrosine phosphorylation led to a decrease in Crn7 abundance in the membrane fraction.

There are several conserved tyrosines in the protein sequence that might be the targets for phosphorylation. Y738 is conserved among both Crn7, POD-1, Dpod-1 and mammalian coronins 2A and 3, Y712 is conserved in Crn7, and both POD-1 proteins. Several other tyrosine residues are present in Crn7 and one or several coronins or POD-1 proteins.

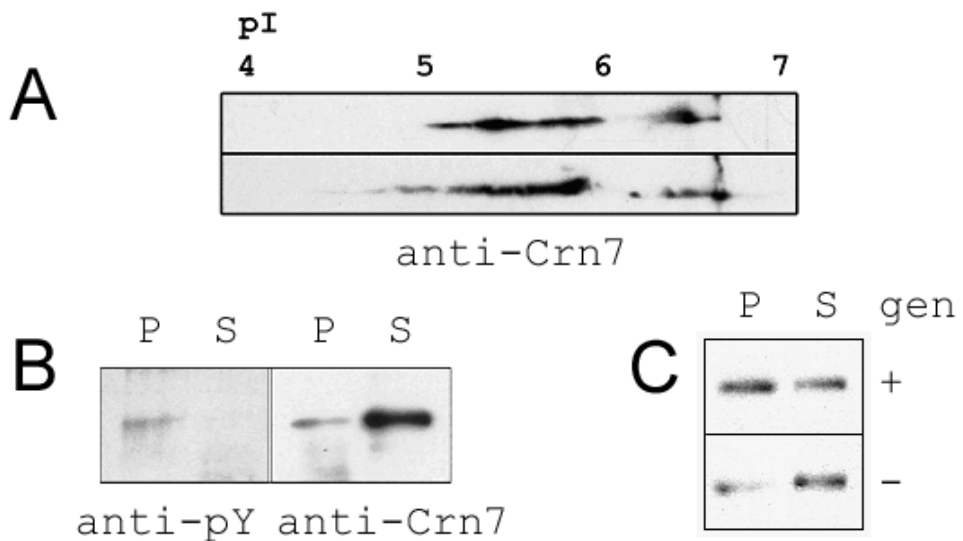


Fig. 12. Crn7 present in the membrane pellet of HeLa cells is phosphorylated on tyrosine residues. A, two-dimensional gel electrophoresis of the proteins present in the 10,000g supernatant and pellet. After separation, the gel was blotted onto a nitrocellulose membrane and probed with Crn7 antibody. B, analysis of tyrosine phosphorylation of the Crn7 protein. The protein was immunoprecipitated from the 10,000g pellet (P) and supernatant (S) using Crn7 antibody. After separation, the gel was blotted onto the nitrocellulose membrane and probed with anti-phosphotyrosine (left) or anti-Crn7 (right) antibody. C, Tyrosine phosphorylation is required for the Crn7 targeting to membranes. Application of tyrosine kinase inhibitor genistein lowers the amount of Crn7 in the membrane pellet (P).

3.4. Analysis of Crn7 function by RNAi

3.4.1. Use of siRNA duplexes to silence Crn7

To reveal the *in vivo* function of Crn7 in the Golgi, we used the small interfering RNA (siRNA) methodology allowing a specific and powerful knockdown of the mRNA and corresponding protein (Novina and Sharp, 2004). We used eight siRNA oligonucleotides (see Methods). 48 and 72 h after transfection, cells were harvested and analyzed by Western blotting.

All siRNA constructs were capable of downregulating Crn7 protein at both treatment terms (Fig. 13A). As the construct siRNA(8)₂₄₅₄ consistently showed the highest degree of downregulation after 48 and 72 hrs, this construct was used in further experiments. siRNA timescale experiments demonstrated that knocking down Crn7 mRNA and protein leads to a dramatic decrease in cell viability, as compared to mock-transfected cells. This effect was both time- and concentration-dependent (Fig. 13B). Thus, Crn7 is an essential protein in HeLa cells.

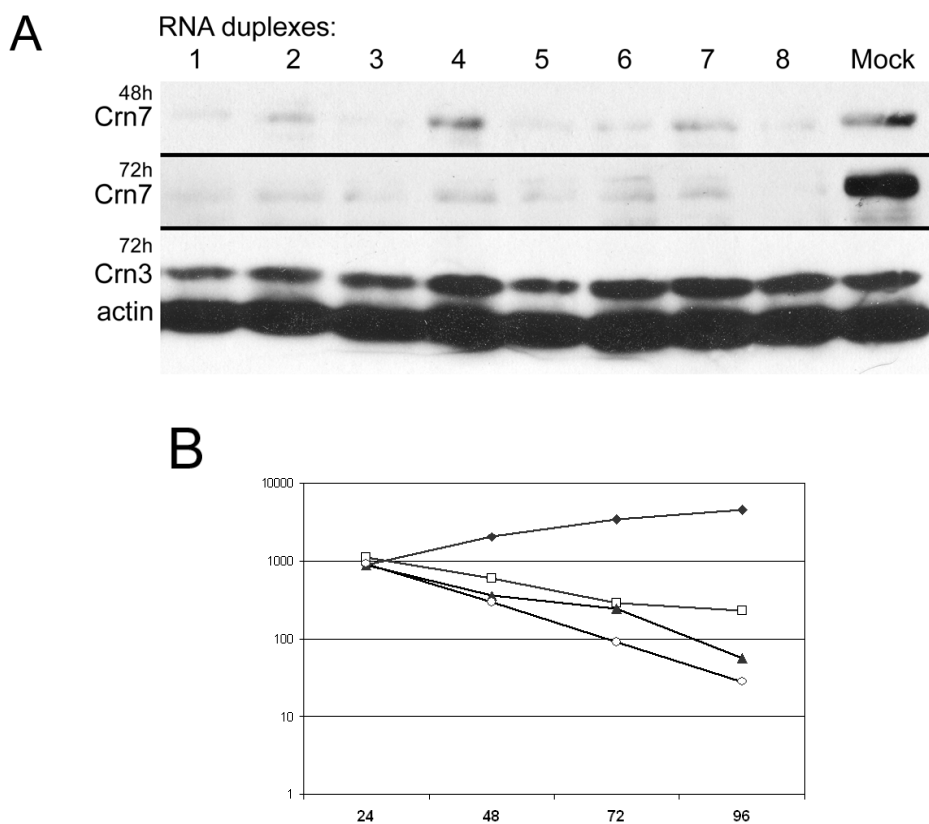


Fig. 13. Downregulation of Crn7 by RNAi results in reduced cell viability and profound changes in Golgi architecture. A, The use of eight individual RNA duplexes to downregulate Crn7 (see Methods). Upper panel, 48 h of RNAi application, Western blot using Crn7 antibody. Middle panel, 72 h of RNAi application, Western blot using Crn7 antibody. Lower panel, 72 h of RNAi application, Western blot using a mixture of coronin 3 (Crn3) and actin antibodies. B, Reduced cell viability upon the application of Crn7 siRNA(8)₂₄₅₄. Filled diamonds, mock-transfected cells, open squares, 1.5 nM siRNA, filled triangles, 5 nM

siRNA, open circles, 15 nM siRNA. Cells were counted 24, 48, 72 and 96 h after the application of siRNA.

Note logarithmic y-scale.

3.4.2. Influence of Crn7 RNAi on the Golgi architecture

To evaluate the effect of Crn7 knockdown by RNAi on the architecture of the Golgi complex, we treated HeLa cells with siRNA(8)₂₄₅₄ for 24 h and processed them for electron microscopy along with mock-treated cells as described in Methods. Mock-transfected cells displayed the expected Golgi morphology, characterized by the presence of several flat cisternae surrounded by transport intermediates (Fig. 14, left). In contrast, HeLa cells treated with siRNA(8)₂₄₅₄ demonstrated different degrees of the Golgi scattering. In most cells, the Golgi was present as a dense accumulation of vesicles still containing one or several cisternae-like structures (Fig. 14, right). In the most extreme cases, no cisternae are observed, and the density of Golgi remnant vesicles decreases. These data suggest that Crn7 is indeed required for the maintenance of the Golgi stability.

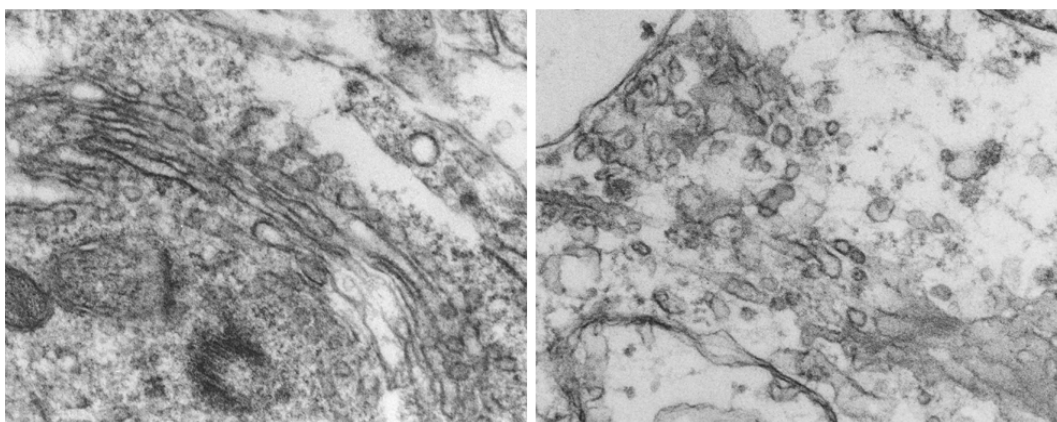


Fig. 14, Ultrastructure of the Golgi complex in mock- (left) and Crn7 siRNA-transfected (right) cells.

Bars, 100 nm.

To better understand the effect of Crn7 knockdown on the Golgi architecture, we studied the distribution of cis- and the trans-Golgi markers in fixed mock- and Crn7 siRNA-transfected HeLa cells (Fig. 15). After 24 h of RNAi application, the Golgi ribbon was not present anymore, and smaller Golgi fragments were scattered in the perinuclear area. The trans-Golgi protein TGN38 and the cis-Golgi marker GM130 were still present in predominantly non-overlapping domains localized close to each other, some of them being organized in ministacks (Fig. 15, right), reminiscent of those forming upon nocodazole treatment (Trucco et al., 2004). Importantly, we could not register any vesicles positive of TGN38 in Crn7 RNAi cells. The absence of TGN38 carriers combined with the accumulation of TGN38 in the Golgi remnants rather than at the cell periphery indirectly indicates an RNAi effect on anterograde, but not retrograde transport of TGN38. At later RNAi terms, the overall structure of the cis-Golgi did not further change, but the trans-Golgi collapsed completely, and TGN38 was only labelling several round-shaped dense compartments per cell (not shown).

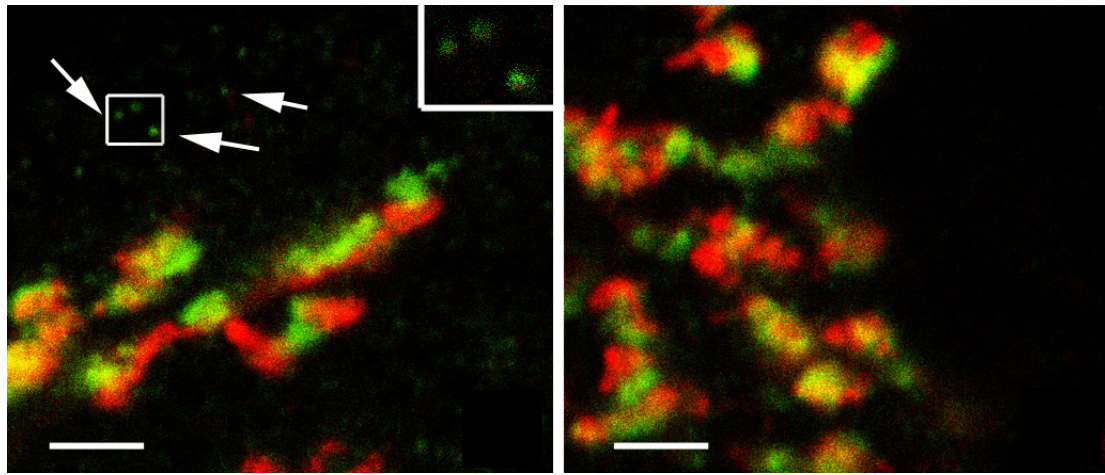


Fig. 15. Mock- (left) and Crn7 siRNA-transfected HeLa cells stained with GM130 (red) and TGN38 (green) antibodies. Note TGN38 carrier vesicles (arrows, and a magnification inserted in E, corresponding to the highlighted area). Size bars, 2 μ m.

3.4.3. Block of protein export from the Golgi in Crn7 RNAi cells.

As we found the formation of TGN38 carrier intermediates to be blocked upon the Crn7 knockdown, we wanted to know whether such effect of Crn7 downregulation on the Golgi export can be reproduced and quantified using the VSV envelope G glycoprotein. VSVG is known to hijack the anterograde transport system to reach the cell surface after proceeding through the ER and Golgi. A VSVG-tsO45 mutant carries a single point mutation F204S (Gallione and Rose, 1985) rendering it temperature-sensitive with regard to its intracellular trafficking. The mutant protein can be accumulated in the ER at 39.5°C, and released to the Golgi complex upon temperature switch to 32°C (see Methods). This mutant is widely used to study the dynamics of protein trafficking along the biosynthetic pathway (Hirschberg et al., 1998; Presley et al., 1997).

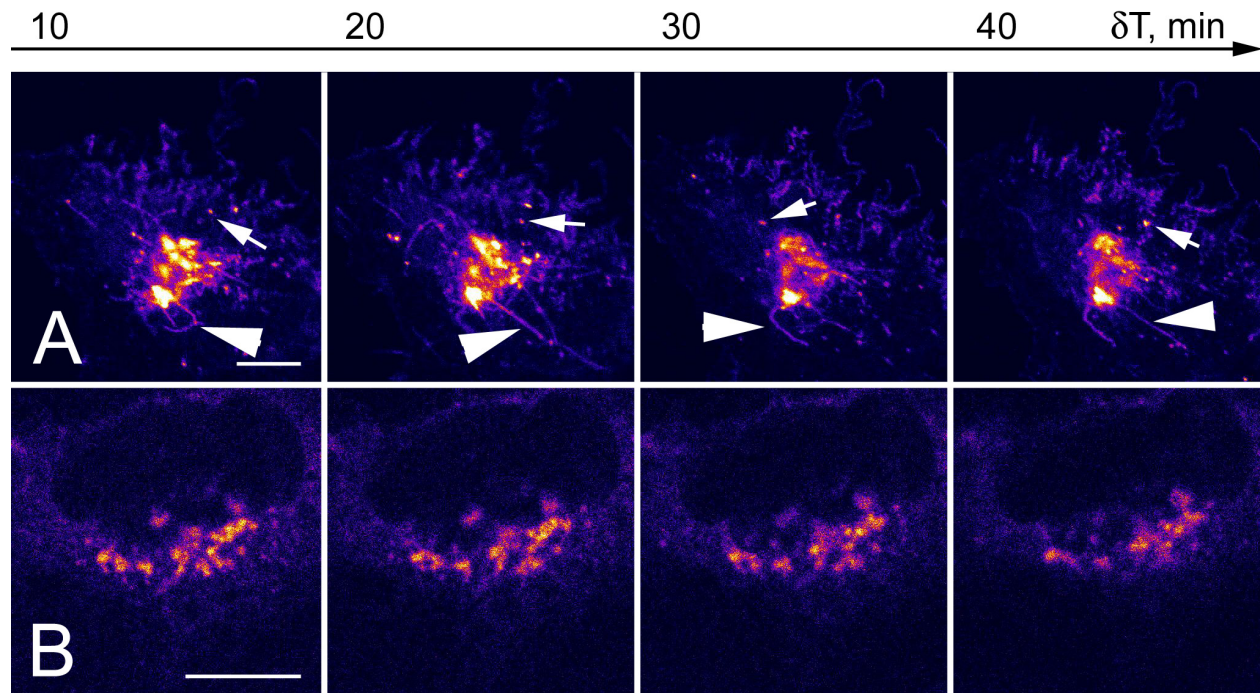


Fig. 16. Block of Golgi export in Crn7 RNAi HeLa cells. Cells were transfected in liquid phase with siRNA and plated for 14 hrs at 37°C, then transfected with VSVG-GFP, kept at 37°C for 2 hrs and at 39.5°C for 8 hrs. For imaging, cells were kept at 32°C to allow VSVG exit from the Golgi. A, Export of GFP-VSVG-tsO45 from the Golgi complex in a mock-transfected cell. Note the formation of Golgi-to-

plasma membrane carriers (arrowheads) and Golgi-derived vesicles (arrows). B, Stability of VSVG-GFP signal pattern in a Crn7 RNAi cell. Note the absence of GPCs and carrier vesicles. Size bars, 10 μm.

In mock-transfected HeLa cells, VSVG-tsO45 gradually accumulated in the Golgi complex upon the temperature shift (not shown). Starting at 10 minutes after the shift, formation of characteristic tubular compartments originating from the Golgi was observed. These intermediates, Golgi-to-plasma membrane carriers (GPC), released vesicles targeted to the plasma membrane (Fig. 16A). Apart from vesicles derived from GPC, we observed direct formation of vesicular transport intermediates leaving the Golgi in the direction of the plasma membrane. Already 10 minutes after the temperature shift, VSVG-tsO45 GFP fluorescence could be observed at the plasma membrane. Cells treated with Crn7 RNAi selected by scattered CFP-GalT pattern and imaged under the same conditions demonstrated a similar rate of accumulation of VSVG in the Golgi apparatus (not shown). However, we did not observe any release of VSVG in GPC or vesicles from the Golgi even 120 minutes after the temperature shift. At all times, the VSVG GFP signal was present in scattered Golgi remnants (Fig. 16B).

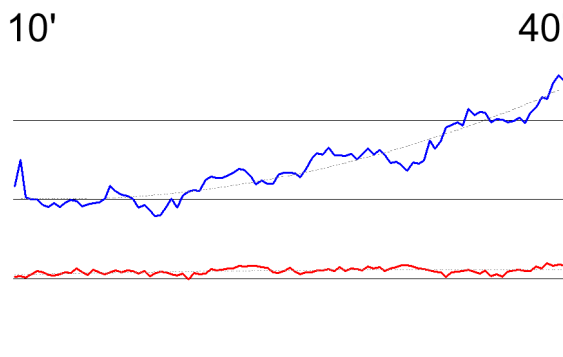


Fig. 17. Relative GFP fluorescence intensity at the plasma membrane of mock-transfected (blue line) and Crn7 RNAi (red line) cells. 100 frames spanning 30 min were quantified. X-axis, time, min; Y-axis, relative GFP fluorescence level at the plasma membrane.

These data infer that the cargo exit from the Golgi complex is completely blocked by Crn7 knockdown. To prove this finding, we measured the VSVG-GFP signal at the plasma membrane in 100 images spanning 30 minutes of time in mock-transfected and Crn7 RNAi cells using MetaMorph software. Fig. 17 demonstrates that in control cells, the GFP fluorescence gradually increases to nearly double the initial value, reflecting the delivery of VSVG from the Golgi complex, whereas in RNAi cells, the GFP fluorescence at the plasma membrane remains at basic threshold level, which is twice lower than that of mock-transfected cells.

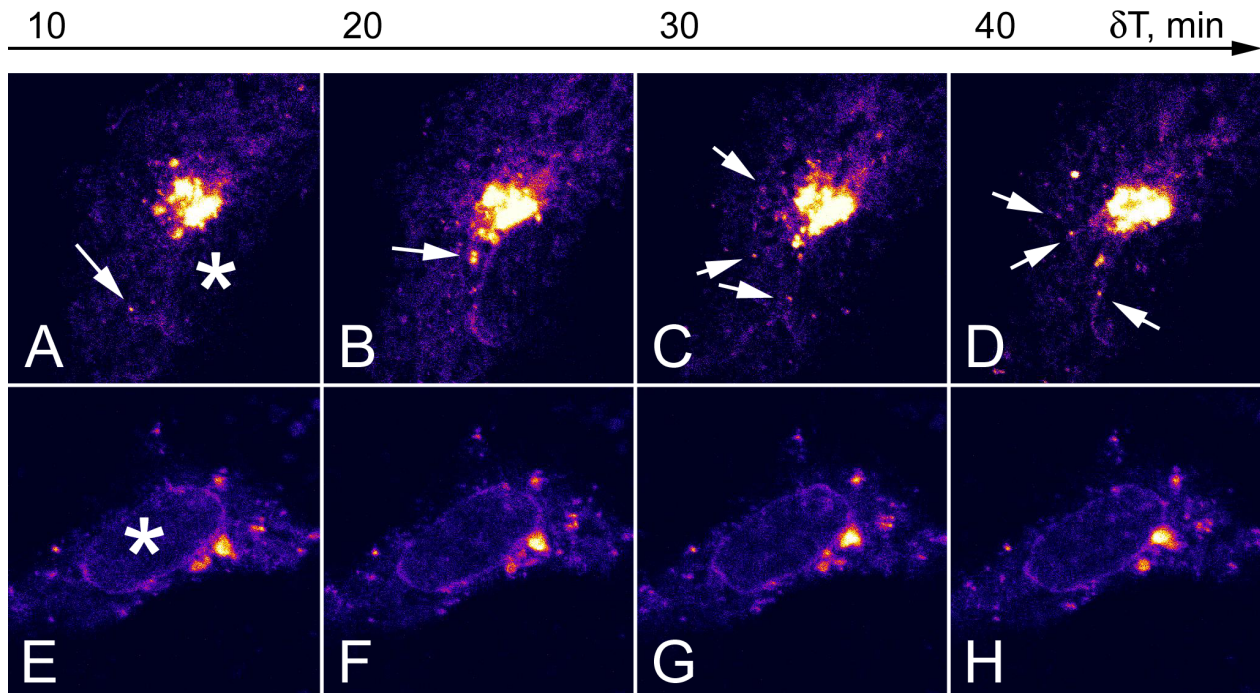


Fig. 18. Block of Golgi export in Crn7 RNAi Vero cells. Experimental conditions as in Fig. 17. A-D, Export of GFP-VSVG-tsO45 from the Golgi complex in a mock-transfected cell. Note the formation of Golgi-derived vesicles (arrows). E-H, Stability of VSVG GFP signal pattern in a Crn7 RNAi cell. Note the absence of GPCs and carrier vesicles. Cell nuclei are marked with asterisks (A, E). Size bars, 10 μ m.

The block of Golgi export was also observed in Vero cells. This cell line is characterized by the delivery of VSVG-tsO45 to the plasma membrane exclusively in Golgi-derived vesicles rather than GPC (Fig. 18A-D). The fact that VSVG export was also blocked in Vero cells (Fig. 18E-H) implies that it is not the cargo progression, but rather cargo selection defect that leads to the export block in both HeLa and Vero cells, as physical movement of vesicles and membrane evaginations require fundamentally different machineries.

We further utilized the vector-based RNAi strategy to follow long-term effects of Crn7 downregulation. DNA fragments encoding siRNA hairpins were cloned into a pSilencer3.1 vector according to manufacturer's guidelines, and HeLa cells were transfected with resulting plasmids. Cells were kept in culture without selection, fixed and processed for immunofluorescence. Knockdown was assessed by Crn7 staining. After one week of vector-based RNAi, dramatic changes were seen in the Golgi structure. As shown by TGN38 staining (Fig. 19A-C), the trans-Golgi was collapsed. Most interestingly, we have observed a strong lysosomal phenotype. In Crn7 RNAi(VB) cells, we could not register any cytoplasmic lysosomes, and the LAMP1 staining was restricted to the Golgi zone (Fig. 19D-F). This implies that the defects in surface-targeted trafficking of TGN38 and VSVG are also characteristic for the lysosomal delivery pathway.

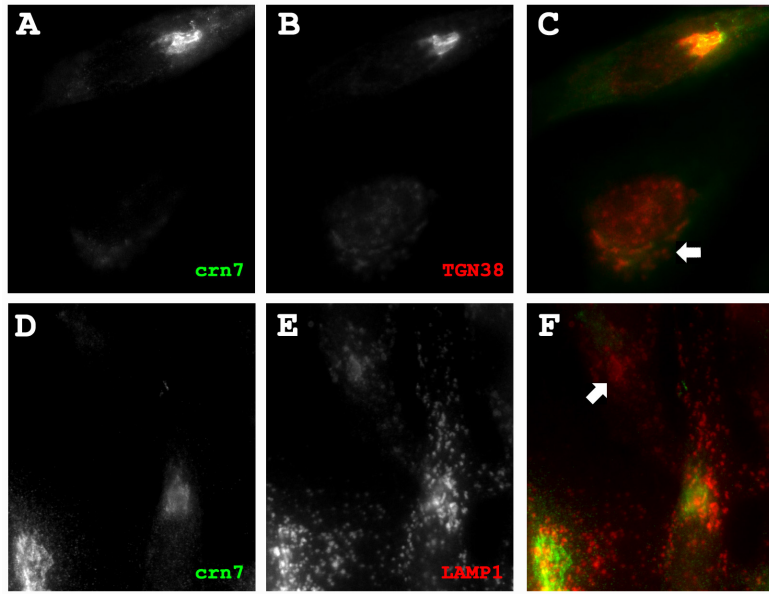


Fig. 19. Localization of TGN and lysosomal markers in HeLa cells transfected with pSilencer3.1 vector encoding Crn7-targeting siRNA. A-C, cells stained with Crn7 (green) and TGN38 (red) antibodies. Note scattered TGN38 staining in a Crn7 knockdown cell (arrow). D-F, cells stained with Crn7 (green) and LAMP1 (red) antibodies. Note the absence of cytoplasmic LAMP-1 structures in the cytoplasm of the Crn7 knockdown cell (arrow), and the accumulation of LAMP-1 in the Golgi area.

We established that the anterograde transport through the biosynthetic pathway is blocked at the Golgi export stage upon downregulation of Crn7. We were interested whether the Golgi import, along with the export, relies on Crn7. That the Golgi entry in anterograde direction is not affected by Crn7 RNAi is evident from the accumulation of VSVG in the Golgi (Figs. 16, 18).

There is another Golgi entry route. A retrograde trafficking pathway connects the endosomal system with the TGN. To test whether the Golgi import from the endosomal system requires Crn7, we compared the intracellular dynamics of CTxB, a non-toxic B-subunit of the cholera toxin (Sandvig et al., 2004). In control cells, Alexa633-labeled CTxB (CTxB-633) was

internalised by cells, and reached the Golgi complex approx. 30 minutes after the beginning of treatment (Fig. 20), well in agreement with literature data. CTxB-633 treatment of Crn7 RNAi cells resulted in a comparable rate of its delivery to the scattered perinuclear Golgi remnants (Fig. 20). Thus, the dynamics of the TGN protein import do not rely on the presence of Crn7 on the cis-Golgi membranes.

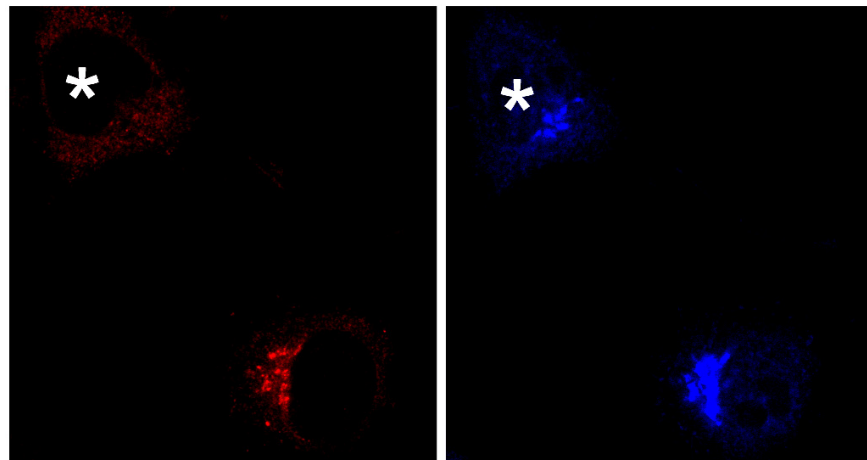


Fig. 20. CTxB delivery to the Golgi complex is not affected by the Crn7 knockdown. Left, Crn7 antibody staining; right, Alexa633-CTxB signal. Note the accumulation of CTxB in the Golgi zone of the cell lacking Crn7 (asterisk).

Our results clearly indicate that Crn7 affects the mammalian Golgi architecture and its function in anterograde protein transport, but not retrograde transport. Based on the localization of the protein at the outer side of the cis-Golgi membrane, we assume that its function can hardly be directly associated with the cargo processing. We anticipate that Crn7 may provide a link between transmembrane cargoes (cargo receptors) lacking own adaptor-interacting sequences with adaptor proteins. Directly downstream of each coronin core domain, the Crn7 protein harbors a copy of a classical YxxΦ motif, known to directly interact with μ -chains of AP adaptor

complex species (Robinson, 2004). Because the Crn7 core domains consist of WD repeats, well known promiscuous protein interaction modules, we anticipated that they may act as cargo- or cargo receptor-binding sites. Disconnection of this link should lead to the accumulation of cargoes in the cis-Golgi.

To address this hypothesis, we tested whether Crn7 is capable of interacting with adaptor protein complexes. We performed immunoprecipitation experiments using α - and γ -adaptin antibodies recognizing parts of AP-2 and -1 adaptor complexes, respectively. Crn7 could be pulled down by the antibody against γ -adaptin, but was not precipitated by α -adaptin antibody (Fig. 21), inferring its interaction with AP-1, but not AP-2. Thus, it does interact with the sorting machinery facilitating the Golgi exit of many cargo proteins. It remains to be established whether WD repeats in the Crn7 core domains are capable of interacting with cytosolic portions of cargo proteins.

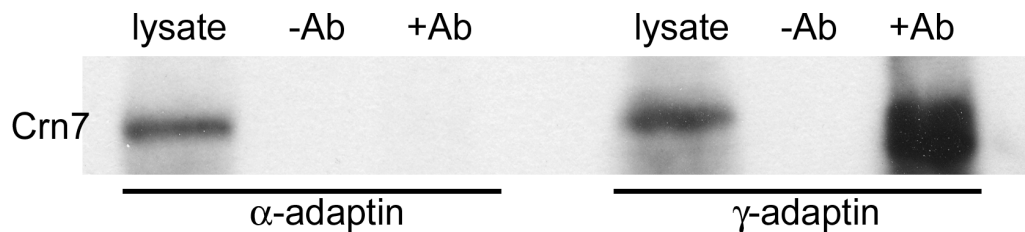


Fig. 21. Crn7 is found in a protein complex immunoprecipitated by γ , but not α -adaptin antibody. Left, detection of Crn7 in total HeLa cell lysate (left), protein A-sepharose beads incubated with HeLa cell lysate in the absence (middle) or presence (right) of the α -adaptin antibody. Right, detection of Crn7 in total HeLa cell lysate (left), protein A-sepharose beads incubated with HeLa lysate in the absence (middle) or presence (right) of the γ -adaptin antibody.

4. DISCUSSION

The Golgi complex is the central protein sorting organelle in eukaryotic cells. The Golgi architecture varies significantly between species and cell types, but the organelle executes principally the same function. Upon the cargo protein entry from the endoplasmic reticulum, resident Golgi enzymes modify the cargo in a way that proteins destined to take different transport routes can be biochemically distinguished between and selectively recruited to the corresponding export carriers. We suggest that Golgi-localized Crn7 can function by regulating the cargo export from the Golgi, and thus affect protein sorting and trafficking along the biosynthetic pathway. We anticipate that Crn7 is recruited to the Golgi membranes by cytosolic portions of non-YxxΦ cargoes and cargo receptors, and interacts with AP-1 to allow the Golgi export of such cargoes/receptors.

4.1. Physical structure and inheritance of the Golgi complex.

The mammalian Golgi complex is one of the largest cellular organelles. In the majority of cells the interphase Golgi is present in form of a single wide perinuclear ribbon comprised of several flattened membrane cisterns, typically around seven and minimally three in number (Fig. 22). Neighboring the two Golgi poles are cis- and trans- Golgi networks (CGN or cis-Golgi and TGN, respectively), the tubulovesicular continua acting as Golgi input and output portals. While cis-Golgi receives biosynthetic input from the endoplasmic reticulum, the TGN is a final sorting organelle. As an organelle, the Golgi complex is polarized physically and biochemically (see below). Cis-, medial and trans-cisternae can be defined according to their morphology, protein composition and function. In mammalian cells, all three parts of the Golgi complex are packed

into the common ribbon and intimately being connected by means of tubular membrane intermediates upon the formation of a trafficking wave (Trucco et al., 2004, and Fig. 22).

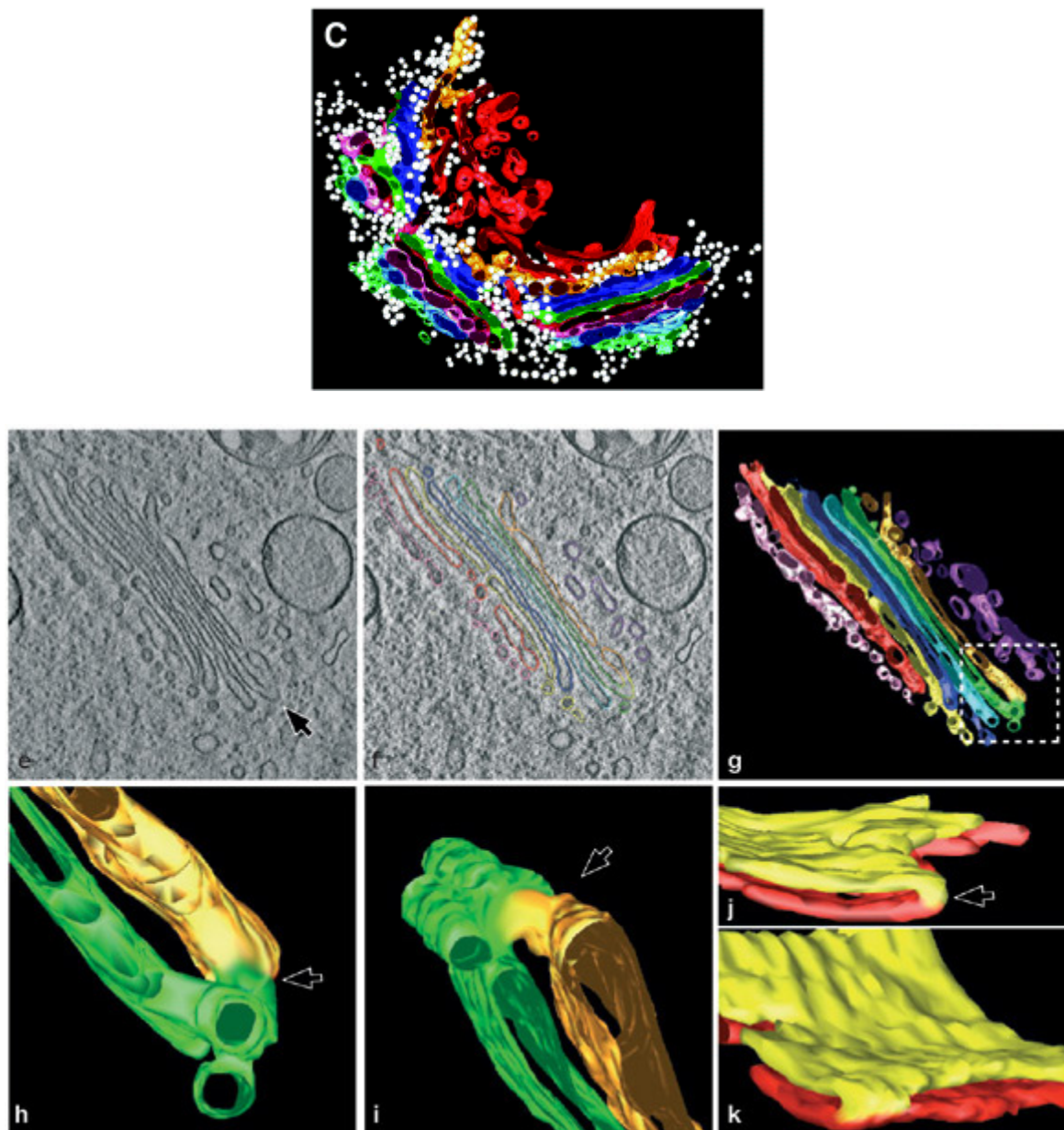


Fig. 22. The mammalian Golgi complex. Top panel, a reconstruction of a typical mammalian Golgi ribbon, as seen by EM tomography. Individual cisternae are shown in green to red, COP vesicles – in white (from Mogelsvang et al., 2004). Bottom panel, reconstruction of serial EM tomography images

demonstrates a formation of direct membrane channels (arrows) connecting individual cisternae upon the induction of trafficking wave. Individual cisternae are shown in red to purple (from Trucco et al., 2004).

The Golgi undergoes dramatic structural changes during mitosis (Rossanese and Glick, 2001). In the early prophase, the Golgi complex is broken down into a “haze”, a collection of clusters, vesicles and small cisternae of different size spread around the cytoplasm (Fig. 4.1.C). Dispersal of the Golgi complex is considered to be required for proper division of its subcomponents between daughter cells. This process is dependent on Polo-like kinase (Lin et al., 2000; Sutterlin et al., 2001) and Mitogen-activated protein kinase kinase I MAPKK or MEK1 (Acharya et al., 1998; Colanzi et al., 2000). At a later stage, Golgi material is further dispersed, and few or no pronounced Golgi structures are distinguishable by light microscopy (Jesch and Linstedt, 1998; Zaal et al., 1999). This process relies on another kinase, Cdc2, but not MEK (Lowe et al., 1998). Shortly after cytokinesis, the Golgi reassembly takes place, relying on a common membrane fusion machinery - NSF, SNAP and p97 (Acharya et al., 1995; Rabouille et al., 1995), as well as on certain resident Golgi proteins like p115, GRASP55 and others (Rossanese and Glick, 2001; Shorter and Warren, 1999; Shorter et al., 1999). The distinct Golgi ribbon is later reconstructed by directed microtubule-based transport of pre-formed Golgi clusters (Moskalewski and Thyberg, 1992; cited after Rossanese and Glick, 2001).

Apparently, although the cellular distribution of Golgi markers at late stages of the mitotic Golgi disassembly resembles that of ER components, and these even often co-localize, the two compartments nevertheless preserve their structural identity throughout the cell cycle. Elegant experiments performed by several groups provided solid evidence that Golgi membranes do not fuse to the ER at any stage of the cell cycle (Axelsson and Warren, 2004; Jesch and Linstedt, 1998; Jokitalo et al., 2001; Pecot and Malhotra, 2004; Terasaki, 2000).

In the yeast *S. cerevisiae*, small single cisternae are scattered around the cytoplasm, usually in a close proximity of cytoskeletal elements. Cis-, medial and trans-Golgi cisternae are not packed together and can be spatially far separated. The perinuclear ribbon is never formed, and there are no direct membrane intermediates connecting individual cisternae. Mitotic inheritance of the Golgi complex in *S. cerevisiae* relies on myosin V-dependent transport of individual cisternae to the forming bud along the actin cables (Rossanese et al., 2001).

4.2. Protein import and progression in the Golgi.

The total protein output from the endoplasmic reticulum is destined to reach the Golgi complex at its cis-pole. The biochemistry of cargo selection in the ER is not yet understood. It is however generally accepted that transport between the endoplasmic reticulum and cis-Golgi pole is mediated by COPII-coated vesicles. COPII coatomer consists of five proteins, Sec23/24, Sec13/31 and Sar1 GTPase (Sec13 being a WD-repeat protein). Type II coatomer assembly is restricted to the ER membrane as activation of Sar1 to Sar1-GTP requires an ER-membrane bound GEF Sec12 (Barlowe, 2002; Springer et al., 1999). Selective recruitment of cargo into the COPII carriers mediating ER-to-Golgi transport can be based on cargo interaction with the COPII coat through diacidic ExD amino acid motifs or pairs of hydrophobic residues like FF or LL (Barlowe, 2002). Cargo proteins have been shown to interact either with Sar1 or Sec24 (Aridor et al., 1998; Belden and Barlowe, 2001a; Belden and Barlowe, 2001b; Dominguez et al., 1998; Giraudo and Maccioni, 2003; Springer and Schekman, 1998; Votsmeier and Gallwitz, 2001).

In the lumen of the Golgi complex, cargo proteins undergo subsequent glycosylation, sugar moieties acting as sorting signals for further progression along the biosynthetic route. Golgi glycosyltransferases are strictly compartmentalized, and their action is achieved by sequential presentation of cargo proteins transported through the Golgi system to different enzymes. Initial

steps of cargo protein glycosylation are taken while still in the lumen of the endoplasmic reticulum. ER glycosylation is important for proper folding of the cargo and for successful transition through the ER quality control system (Buck et al., 2004; Shi and Elliott, 2004; Vuillier et al., 2005; Wujek et al., 2004).

4.3. Golgi export.

Export from the Golgi complex is based on the interaction of cargo molecules or cargo receptors with cytosolic sorting machinery elements, such as GGA proteins and AP (adaptor protein) complexes. GGA proteins 1-3 are known to directly interact with the mannose-6-phosphate cargo receptors (MPR) and hand them over to adaptor proteins in forming clathrin vesicles for the Golgi export (Bonifacino, 2004; Gleeson et al., 2004). AP complexes are heterotetramers consisting of subunits called adaptins. They participate in vesicular trafficking between different cellular organelles (Figs. 23, 24).

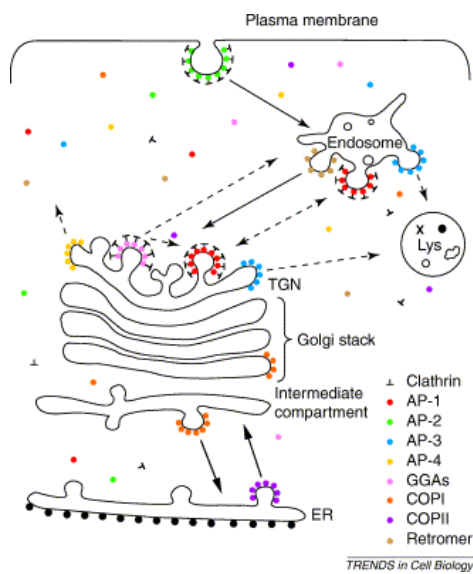


Fig. 23. Membrane specificities of AP and GGA proteins (from Robinson, 2004).

In case of AP-1, the complex is constituted of two large subunits, γ and $\beta 1$, a medium $\mu 1$ and a small $\sigma 1$ subunit. β -adaptins are known to interact with clathrin (Ahle and Ungewickell, 1989; Dell'Angelica et al., 1998), and, along with α - and γ -adaptins, to bind several accessory proteins (Page et al., 1999; Slepnev and De Camilli, 2000). μ -subunits of AP complex tetramers in turn interact with YxxΦ motifs of cargo proteins (Ohno et al., 1995). Another sorting motif known to be recognized by AP complex proteins is a dileucine signal, interacting with γ - and δ -subunits of AP-1 and -3 (Janvier et al., 2003).

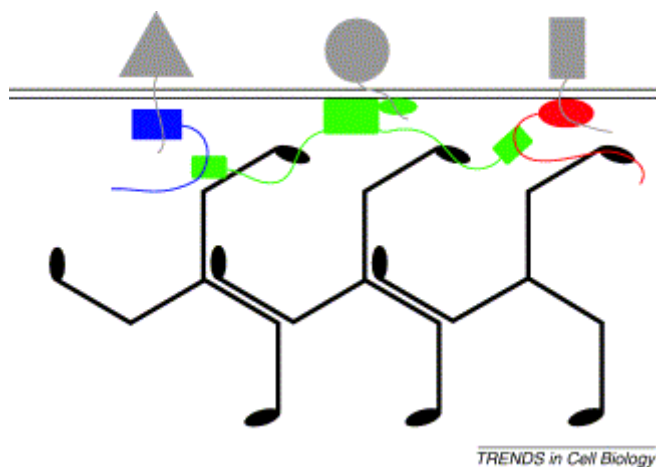


Fig. 24. Adaptor proteins (in color) connect Golgi cargoes (top) to clathrin (bottom). Green, the AP-1 recognizes a YxxΦ-containing cargo and interacts with clathrin and other adaptors (blue and red). Numb-like adaptors (blue) can bind cargoes but require AP-1 to connect to clathrin. Epsin-like adaptors (red) can bind both cargoes and clathrin. The formation of the clathrin coat is based on a first level protein network formed by adaptors connected to sorting signals of cargo proteins. (Robinson, 2004).

Recognition of sugar trees and protein sorting into distinct export routes takes place at the trans-Golgi pole and in the TGN. It is best understood in case of the lysosomal pathway based on mannose-6-phosphate receptor (M6PR) function. In brief, M6PR recognizes sugar moieties specific for proteins destined to be transported to the endolysosomal system. Ligand-bound

receptors clusters are packed into clathrin-coated vesicles, probably depending on Golgi-localized, γ -earcontaining, Arf-binding (GGA) family of proteins family proteins (Puertollano et al., 2001a; Puertollano et al., 2001b).

4.4. Models of Golgi dynamics.

Protein sorting in the Golgi requires constant cargo progression through the ribbon from its cis- to trans-pole allowing sequential modification of glycoprotein sugar moieties. At least three distinct hypotheses were proposed in order to explain how the cargo flow progresses through the Golgi complex (reviewed in Griffiths, 2000; Elsner et al., 2003).

- According to the **vesicular trafficking** model, the Golgi cisternae are stable immobile compartments maintaining constant enzyme compositions. Cargo protein progresses through the stack by sequential retrieval into carrier vesicles connecting individual cisternae. Retrograde flow is required to achieve membrane homeostasis.
- The **cisternal maturation** theory suggests that tubulovesicular carriers derived from the endoplasmic reticulum gradually fuse to form the cis-most cistern that is later displaced in the trans-direction by the cistern to form next. Maintenance of Golgi enzyme compartmentalization is achieved by constant retrograde vesicular traffic returning the resident Golgi material to the proper cistern.
- The most recent model suggests that protein trafficking through the Golgi stack relies on formation of **transient connections** between neighboring cisternae. Such membrane channels allow immediate unidirectional cargo flow from one cistern to another.

The last two models have been initially based on an assumption that many cargoes are too bulky to be packed into small carrier vesicles. Examples of such cargoes are surface scales produced by algae or vertebrate procollagens (Melkonian et al., 1991; Bonfanti et al., 1998).

Probably the best understood anterograde trafficking model system utilizes ts045-VSVG, the thermostable variant of the vesicular stomatitis virus G-glycoprotein (VSVG; Gallione and Rose, 1985). Under standard conditions, cultured cells stably or transiently expressing ts045-VSVG transport the glycoprotein from the ER to the cell surface through the Golgi complex. However, upon the temperature shift to 40°C, the same cells accumulate the glycoprotein in the ER, and within approx. 20 hrs of incubation in this conditions, ts045-VSVG is present in bulk amounts exclusively in the ER (Presley et al., 1997; Hirschberg et al., 1998). Lowering the temperature to 32 degrees releases a massive synchronized wave of ts045-VSVG from the ER to the Golgi complex and downstream compartments allowing to precisely assess trafficking dynamics of this process. This system was utilized successfully to study protein trafficking between the endoplasmic reticulum and Golgi (Presley et al., 1997) and between the Golgi complex and the plasma membrane (Hirschberg et al., 1998). A recent study utilized a VSVG trafficking wave to assess the intra-Golgi trafficking mechanics (Trucco et al., 2004). Using separated stacks derived from the Golgi ribbon upon nocodazole treatment, Trucco et al. were able to directly demonstrate by electron microscopy tomography that induction of a VSVG wave results in development of transient intercisternal connections bridging the adjacent cisterns. This finding provided the first experimental evidence for the transient connections model that remained purely theoretical until then.

The same group earlier demonstrated that Golgi enzymes are not present in COPI vesicles mediating retrograde membrane flow within the Golgi stack and between the Golgi and ER (Kweon et al., 2004). This evidence together with other (Orci et al., 2000a, b) is however in odds

with data obtained by other groups (Lanoix et al., 2001; Martinez-Menarguez et al., 2001) showing clear accumulation of resident Golgi proteins in COPI carriers. This discrepancy is probably due to using different cell types, cargo models and experimental conditions. It is reasonable to argue that in most cases, protein trafficking through the Golgi occurs as a combination of vesicular trafficking and direct intercysternal bridging events.

4.5. Crn7 is a novel WD-repeat protein localized to the Golgi complex.

Coronin family proteins have been shown to regulate the cytoskeleton in a variety of systems (see Introduction). A systematic database research was earlier performed in the laboratory (A. Schulze, Diploma thesis, University of Cologne, 2001) to find out whether the human family is restricted to six 400-500 kDa coronins known previously (reviewed in de Hostos, 1999). An additional putative EST was identified, encoding a protein harboring two typical coronin core domains, as the related *C. elegans* POD-1 and Dpod-1 from *Drosophila* do. A complete cDNA for human Crn7 by reverse transcription PCR was cloned using information from the EST database (A. Schulze, Diploma thesis, University of Cologne, 2001). The sequence encodes a 925-amino acid protein with a predicted molecular weight of 100.5 kDa and a predicted isoelectric point of 5.6. A structural peculiarity of Crn7 is the presence of a 47-amino acid long proline, serine and threonine-enriched stretch preceding the second group of WD repeats designated a PST motif. Crn7 protein is 46% and 47% homologous and 30% and 29% identical to Dpod-1 and POD-1, respectively as predicted by NCBI BLAST server using BLOSUM62 matrix. Phylogenetic analysis using cluster algorithm clearly positions Crn7 and both previously described POD-1 proteins in a group distinct from other coronins. Like both POD-1 proteins, Crn7 does not possess a C-terminal coiled coil dimerization domain typical for short coronins.

Our subcellular fractionation data strongly infer that the protein is distributed between cytosol and membrane fractions. The bulk of the protein is present in the cytosol, where almost equal proportions are found in a free state or in small protein complexes (200,000g supernatant) and in large complexes (200,000g pellet). Separation of postnuclear supernatants on sucrose gradients resulted in two prominent peaks of Crn7, corresponding to approx. 10-15% and 40-50% of sucrose suggesting that the protein is present in two distinct compartments. These data are in good agreement with differential centrifugation results implying that Crn7 is localized on both light and heavy membranes. Immunofluorescent analysis of fixed permeabilized cells demonstrated that the bulk of membrane-associated Crn7 is localized in the Golgi complex. By electron microscopy, we could confirm our biochemical and immunofluorescence data by showing Crn7 to be present on the outer side of the Golgi membrane.

4.6. Targeting of Crn7 to the Golgi.

Golgi proteins can be transported to the organelle either via the biosynthetic pathway (luminal and transmembrane proteins) or from the cytosol (peripheral membrane proteins of the outer side). In order to be transported to the Golgi via the biosynthetic route, the proteins in question first arrive in the lumen of the ER. ER import is a multi-step process requiring the docking of a polyribosome synthesizing the polypeptide at the ER membrane, recognition of the newly synthesized hydrophobic amino terminus by the signal recognition particle (SRP), pumping the molecule into the lumen and finally cleavage of signal peptides by the ER signal peptidase. The “rule-of-thumb” in predicting whether the protein in question will or will not be physically capable of being inserted into the ER is that a well-defined hydrophobic N-terminus is absolutely required.

The analysis of Crn7 N-terminus hydrophobicity using SignalP-HM algorithm (available at <http://www.cbs.dtu.dk/services/SignalP/>) demonstrates that although Crn7 does indeed possess weakly hydrophobic amino acid environments close to its amino terminus, still the hydrophobicity values are well below threshold, and a cumulative probability of any region to represent a signal cleavage site is close to zero (Fig. 25).

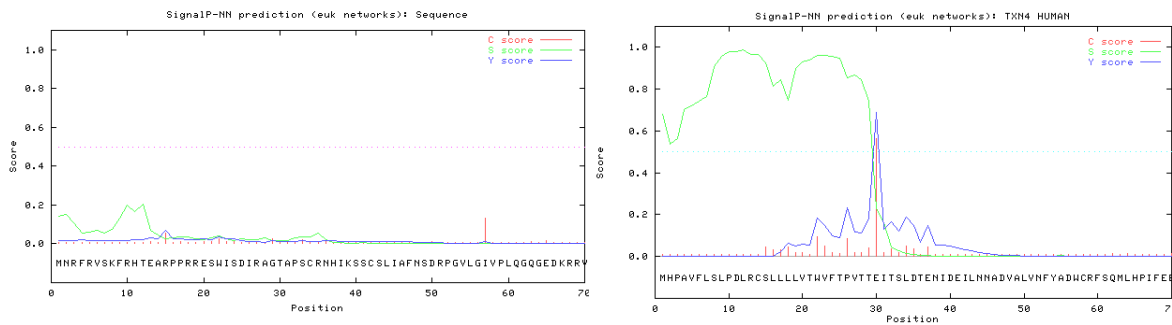


Fig. 25. Analysis of hydrophobicity and signal peptide cleavage site probabilities of Crn7 (left) and a bona fide secretory protein Txn4 (right). Green line, hydrophobicity of individual amino acids starting from the most N-terminal (see sequences below). Red bars, probability of each individual amino acid being the most C-terminal of a cleaved signal peptide. Blue line, cumulative value predicting a border between the most C-terminal amino acid of a signal peptide and the most N-terminal amino acid of the mature secretory protein. Dashed horizontal line, threshold (0.5).

Thus, it is very improbable that Crn7 reaches the Golgi from the ER lumen. This assumption is well in agreement with our biochemical and EM data. Firstly, we showed that Crn7 is found on the outer side of Golgi membranes by electron microscopy (Fig. 8G). Secondly, the protein was shown to be extracted from membrane pellets by treatment with sodium carbonate known to solubilize peripheral membrane proteins, and it could not be protected from proteinase cleavage by compartment membranes. Thus, we conclude that Crn7 is synthesized in the cytosol and attached to the outer side of Golgi membranes.

Now, what drives Crn7 to the Golgi membrane? Our data suggest that it is tyrosine phosphorylation. Not only is Crn7 phosphorylated on tyrosine residues in the membrane fraction, but also interfering with tyrosine phosphorylation using short-term genistein treatment leads to a reduction of Crn7 on membranes. Phosphorylation is an important signal regulating membrane targeting of many proteins. For example, it has been established that phosphorylation dramatically increases the binding of AP-2 adaptors to sorting signals (Fingerhut et al., 2001; Ricotta et al., 2002).

A second requirement for Crn7 attachment to Golgi membranes is the protein import from the ER. We demonstrated that upon short-term overexpression of syntaxin 5, a cis-Golgi t-SNARE known to negatively regulate ER-to-Golgi transport, the amount of Crn7 on Golgi membranes significantly decreased. These findings imply that the Golgi cargoes (short-term storage proteins retrieved from the ER to Golgi) are necessary for the Crn7 targeting to the Golgi.

4.7. Possible function of Crn7 in the Golgi complex.

Our data suggest that Crn7 is attracted to Golgi cargoes in a phosphorylation-dependent manner and interacts with AP-1 complex mediating Golgi export. The Crn7 RNAi phenotype is characterized by the block of Golgi exit of several proteins. TGN38, a Golgi protein cycling between the compartment and the plasma membrane, a lysosomal marker LAMP-1 and an anterograde trafficking model protein VSVG all accumulate in the Golgi and fail to reach their final cellular destinations. Together with the localization pattern, this phenotype suggests that Crn7 is indeed required for the Golgi export of cargoes.

How can such effect be achieved?

A **first** possibility is that in Crn7 knockdown cells Golgi cargoes are not properly modified (e.g. glycosylated) in a way that is required for export. For example, lack of mannose

residues attached to luminal Golgi cargo molecules might in principle affect cargo recognition by mannose-6-phosphate receptors and the subsequent interaction between M6PR and the sorting machinery required for export. However, direct participation of Crn7 in glycosylation in the Golgi would require the presence of Crn7 in the lumen of the Golgi/ER system, which is indeed not the case.

A **second** possibility is that Crn7 is a co-adaptor linking cargoes or cargo receptors to the AP complex species to facilitate the export. Such bipolar interaction may, for example, assist cargoes lacking their own sorting signals to be linked to AP. To execute such a function, Crn7 would have to (a) bind transmembrane cargoes (receptors), and (b) interact with AP-1 or -3 or -4, adaptors present in the Golgi. Although we did not demonstrate any direct interaction between Crn7 and cargoes, we were able to establish that it does require cargo efflux for its Golgi localization, as interfering with cargo entry by overexpressing Syn5 dramatically reduced the amount of Crn7 on the Golgi membranes. On the other side, we clearly demonstrated the interaction of Crn7 with AP-1, but not AP-2.

Importantly, there is no indication that any known AP complex species (AP-1 – AP-4) or GGA proteins mediates direct transport between the Golgi complex and the plasma membrane (see Fig. 23), which is indeed the major Golgi export route taken by surface receptors, components of extracellular matrix and soluble secretory proteins. Thus, the **third** and most speculative way Crn7 may act in the Golgi complex is to take over a role of “AP-5” to connect Golgi cargoes to plasma membrane in a clathrin-dependent or independent process.

4.8. Crn7 is an essential mammalian protein.

Our data suggest that Crn7 is a ubiquitous protein abundantly expressed in most cell types and tissues. RNAi experiments showed that Crn7 knockdown results in dramatic, time- and

concentration-dependent decrease in cell viability. Taken together, these findings imply that the function of Crn7 in the Golgi, e.g. providing the functional connection between Golgi cargoes and export machinery, is indeed biologically significant.

Importantly, not all organisms possess predicted Crn7 homologues. For example, in yeast *S. cerevisiae* there is a single coronin family member, and its function appears to be restricted to Arp2/3-mediated cytoskeleton regulation. Thus, the function of mammalian Crn7 is probably executed by another protein, for example an epsin-like protein (Duncan et al., 2003). An alternative is that yeast cargoes do not require co-adaptors and interact directly with AP-1 and/or GGAs.

In *Drosophila* and *C. elegans*, proteins homologous to Crn7 are present. Importantly, both POD-1s interact with actin and tubulin, in contrast to Crn7. The *C. elegans* POD-1 mutant phenotype might suggest a role in Golgi export as mutant worms display an accumulation of giant vacuoles (Golgi-derived? Swollen Golgi?) in the cytoplasm, and the formation of the eggshell is impaired. However, Golgi localization of the worm POD-1 (Crn7) was never observed. In the case of *Drosophila* Dpod1, the Golgi localization was never observed either.

It is important to emphasize that a wide variety of coronins was probably first established by mammals. Evolutionary older phyla are characterized by the presence of either one (short) or two (one long and one short) coronins. It is reasonable to speculate that the functions of mammalian coronins are more diverse than those of yeast, *Drosophila* or *C. elegans*. Crn7 appears to be unique with regard to its Golgi localization, function and essential nature.

5. MATERIALS AND METHODS

"If you can't do it using imaging, there is no reason for doing it at all..."
- overheard at a conference

Methods not included in this section were standard methods (Sambrook, J., Fritsch, E.F., and Maniatis, T. Molecular Cloning: A Laboratory Manual. Cold Spring Harbor Laboratory Press, NY, Vols. 1-3 (1989). Buffer solutions not described were standard (*ibid.*) Fine chemicals were from Sigma, unless indicated otherwise. Standard laboratory reagents were from local suppliers.

4.1. Acquired Reagents.

Drs. Mark McNiven, Toshitaka Tanaka and Martin Lowe generously provided rabbit polyclonal antibodies against TGN38, LAMP1 and GM130, respectively. Antibodies against Crn7 and Crn3 (monoclonal), β COP and Erd2p (polyclonal) were reported previously (Majoul et al., 1998; Rybakin et al., 2004; Spoerl et al., 2002). GFP-Syn5 was a gift from Drs. Rainer Duden and Irina Majoul. GFP-VSVG(ts-045) plasmid was from Dr. Jennifer Lippincott-Schwartz. Alexa633-labelled CTxB was from Molecular Probes (Utrecht, the Netherlands).

4.2. Mammalian Cell Culture

HeLa, NIH 3T3 and Vero cells were from ATCC. Cells were grown in a Dulbecco's modified Eagle's medium containing 4.5 g/liter glucose (Sigma), supplemented with 10% fetal calf serum (Biochrom), 2 mM L-glutamine (Biochrom), 1 mM sodium pyruvate (Biochrom), 100 U/ml penicillin G, and 100 μ g/ml streptomycin (Invitrogen). For transfections, we used the Lipofectamin Plus system (Invitrogen) or FuGENE6 reagent (Roche) according to the

manufacturers' guidelines. For immunofluorescence, cells were grown on coverslips to approx. 50% confluence, fixed with 3,7% paraformaldehyde, rinsed twice with 20 mM glycine, blocked with 0,045% fish gelatine in the presence 0,2% saponin and incubated with primary antibodies diluted in blocking buffer. Where indicated, brefeldin A or nocodazole were added to the cell culture medium at the indicated concentrations. Latrunculin B was used at 1 µg/ml for 30 min, brefeldin A at 20 µg/ml for 5-120 min, colchicine at 5 µg/ml for 30 min, nocodazole at 33 µM for 30-120 min.

4.3. Protein electrophoresis, immunoblotting, immunoprecipitation.

Protein samples were separated by SDS-PAGE (10% acrylamide) and blotted onto nitrocellulose filters. Unspecific binding of the antibodies was blocked with 4% skimmed milk, 1% BSA in TBS-T (10 mM Tris-HCl, pH 8.0, 150 mM NaCl, 0.2% Tween 20). The following primary antibodies were used: monoclonal anti-Crn7 42-137-1 (hybridoma supernatant) at 1:5, beta-actin specific mAb AC74 (Sigma) at 1:10,000, rabbit polyclonal anti-Rab5 (Transduction Laboratories) at 1:250, anti-phosphotyrosine mAb at 1:50, rabbit anti-phosphoserine / phosphothreonine at 1:1000, rabbit polyclonal anti-PDI antibody (StressGen) at 1:2,000. Horseradish peroxidase-conjugated secondary antibodies against murine and rabbit IgG (Pierce) were used at 1:7500 and 1:10,000, respectively.

Immunoprecipitation using protein A-Sepharose (Amersham) was performed as described (Neubrand et al., 2005). In brief, cells were grown on ten 15-cm plastic dishes until 90% confluence, scraped and homogenized in 1% NP-40 buffer. Lysates were precleared with protein A-Sepharose and incubated with 20 µg of the antibody of interest overnight at 4°C. Protein complexes recognized by the antibody were pulled down by protein A-Sepharose beads. Beads were then washed five times with ice-cold NP-40 buffer and boiled in SDS-PAGE probe buffer.

Mouse monoclonal antibody against γ -adaptin antibody was from Sigma, rabbit polyclonal antibody against α -adaptin was from Santa Cruz Biotechnologies.

4.4. Immunostaining and imaging

The cells were washed briefly with PBS, fixed with 4% paraformaldehyde at room temperature, rinsed with 20 mM glycine and permeabilized with 0.2% saponin in PBS. Saponin was present in the buffers at all later stages of staining at the concentration of 0,02%. Unspecific binding of the antibodies was blocked with 0.045% fish gelatine, 0.5% BSA, in PBS. The following primary antibodies were used: anti-Crn7 mAb 42-137-1 at 1:75, anti-Erd2p polyclonal antibody at 1:50, polyclonal anti-TGN38 at 1:150, polyclonal anti-LAMP1 at 1:50, and polyclonal anti- β -COP at 1:50. Secondary goat anti-mouse antibody conjugated with Cy3 (Sigma) was used at 1:500-1:2000, sheep anti-rabbit antibody conjugated with FITC (BioRad) at 1:1000. Coverslips were mounted in gelvatol and analyzed using fluorescent and confocal microscopes (Leica and Olympus). Digital images were acquired using SensiControl 4.03 software (PCO Computer Optics, Germany). Immunohistochemical analysis was performed on paraffin-embedded 5- μ m sections of paraformaldehyde-fixed murine tissues. The deparaffinized sections were treated with a 1:75 dilution of affinity purified anti-Crn7 antibody overnight at 4 °C and a 1:500 dilution of Alexa 488-conjugated anti-IgG1 secondary antibody (Molecular Probes) for 2 h at room temperature. Sections were counterstained with DAPI and visualized by fluorescence microscopy.

For transferrin uptake experiments, FITC-labelled transferrin (Sigma) was added to the cell culture medium for 10 min on ice at 50 μ g/ml. The cells were then washed and allowed to internalise transferrin for the indicated periods of time at 37°C.

4.5. Subcellular fractionation and two-dimensional gel electrophoresis

Subcellular fractionation experiments were performed as described (Spoerl et al., 2002), except for cell homogenization which was performed by passing the cells through a 21G 1½ needle 15 times. For phosphorylation assays, all the steps were performed in the presence of 1 mM sodium orthovanadate and 25 nM okadaic acid (BioChemika). Separation of membrane organelles on discontinuous sucrose gradients and two-dimensional gel electrophoresis were performed as described (Spoerl et al., 2002).

4.6. RNA interference.

Following short interfering RNA oligonucleotides targeted against human Crn7 were designed and supplied by Qiagen: siRNA(1)₁₂₃, siRNA(2)₊₅₂₀, siRNA(3)₁₄₅₂, siRNA(4)₁₆₃, siRNA(5)₂₆₃₉, siRNA(6)₂₀₅₅, siRNA(7)₊₆₀, siRNA(8)₂₄₅₄. Lower indices indicate the starting positions of the corresponding sequences in the Crn7 mRNA; oligonucleotides 2 and 7 target fragments of the 3' region of Crn7 mRNA starting 520 and 60 bases after the last coding base, respectively. “Fast forward” transfection of HeLa using HiPerFect reagent (Qiagen) was performed according to the manufacturer’s protocol. For immunofluorescence, siRNA were used to transfect 50%-confluent cells on 12-mm (5 nM RNA) or 25-mm (30 nM RNA) coverslips in all experiments. Cells were analyzed 24 or 48 h after transfection. For electron microscopy, 3 nM siRNA were used to transfect 90%-confluent HeLa cells on 12-mm coverslips, and cells were fixed 24 h after transfection. For Western blotting, fresh cells were plated onto 6-well plates at 50% confluency, and analyzed 48 and 72 h after transfection. As controls, mock-transfected and a scrambled RNA-transfected cells were used.

For vector-based RNAi, pSilencer3.1 vector (Ambion) was used. Following sense and antisense oligonucleotides targeting the region of Crn7 coding region positions 106 and 115 were annealed and cloned into pSilencer:

106> 5'-GATCCGCCACATCAAATCAAGCTGCTCAAGAGAGCAGCTTGATTGATGTGGTTTTGGAAA-3'
106< 5'-AGCTTTCAAAAAACCATCAAATCAAGCTGCTCTTGAAGCAGCTTGATTGATGTGGCG-3'

115> 5'-GATCCATCAAGCTGCAGCTTGATCTCAAGAGAGATCAAGCTGCAGCTTGATTTTGGAAA-3'
115< 5'-AGCTTTCAAAAAATCAAGCTGCAGCTTGATCTCTTGAAGATCAAGCTGCAGCTTGATG-3'

The pSilencer plasmid was introduced into HeLa cells as described in 2.3.

4.7. Electron microscopy.

For immunoelectron microscopy, three 25-day old black-hooded Lister rats were used. Animal husbandry and Methods were approved by the Ethics Committee on Animal Experimentation, University of Groningen, the Netherlands. Animals were deeply anaesthetized with sodium pentobarbital (Nembutal^R, i.p., 50 mg/kg) and perfused transcardially, first with a solution containing 2% polyvinylpyrrolidone (MW 30 000), 0.4% NaNO₃ in phosphate buffer (PB; 0.1 M, pH7.4) for 1 min, and then with 4% paraformaldehyde in PB for 10 min. Whole brains were removed and stored overnight in the fixative at 4°C. Fifty-micrometer sagittal sections of the cerebellum were taken using a vibratome. The sections were washed with 0,05 M PB, pH7.4, and incubated sequentially in (1) 1% sodium borohydride in PB (0,05 M, pH7.4) for 30 min; and (2) 25% sucrose and 3.5% glycerol in PB (0,05 M, pH7.4) overnight. Sections were rapidly frozen in liquid propane, washed in 0,1 M PB and incubated with monoclonal anti-Crn7 antibody diluted 1:50 (in PB, with 0.5% BSA, 0.1% coldwater fish gelatine) at 4°C for 48 h (control sections were stained without primary antibodies). The primary antibody was visualized using goat anti-mouse antibody Fab fragments coupled to 5 nm gold particles (Amersham, Arlington Heights, IL). Subsequently sections were equilibrated in 0.1 M cacodylate buffer

pH7.6 and fixed in 2% glutaraldehyde in the same buffer for 30 min. Sections were then osmicated in 1% OsO₄, 1.5% potassium hexacyanoferrate in cacodylate buffer for 15 min, dehydrated in ethanol and embedded in Epon. Serial ultrathin sections were counterstained with uranyl acetate and lead citrate, and examined using a Philips CM 100 transmission electron microscope.

For the electron microscopy analysis of the Crn7 knockdown phenotype, mock- and siRNA-transfected HeLa cells were fixed for 10 min at room temperature in 100 mM PB containing 4% paraformaldehyde and stored at 4°C in PB containing 1% paraformaldehyde until further use. Cells were osmicated, dehydrated and embedded as described above. Ultra-thin sections were cut and counterstained with uranyl acetate and lead citrate.

4.8. VSVG and CTxB trafficking assays.

Trafficking assays were performed essentially as described (Hirschberg et al., 1998; Majoul et al., 1996). In brief, for VSVG trafficking assay, HeLa or Vero cells were co-transfected with GFP-VSVG-tsO45 and CFP-GaIT plasmids, kept at 37°C for 2 hrs, and at 40°C for 16 hrs. Cells were then shifted to 32°C in the presence of 150 µg ml⁻¹ cycloheximide in phenol red-free DMEM high-glucose medium supplemented with 10% serum and 20 mM HEPES to allow the synchronous export of VSVG from the ER. Where indicated, cells were transfected with siRNA 6 h prior to transfection with VSVG. For CTxB trafficking assay, Alexa633-labelled CTxB (from Molecular Probes, 500 ng ml⁻¹) was added to the cell culture medium for 3 min at room temperature, followed by washing, internalisation at 37°C, fixation and immunolabeling.

4.9. Histology.

Immunohistochemical analysis was performed on paraffin-embedded 5- μ m sections of paraformaldehyde-fixed murine tissues. The deparaffinized sections were treated with a 1:75 dilution of affinity purified anti-crn7 antibody overnight at 4°C and a 1:500 dilution of Alexa 488-conjugated anti-IgG1 secondary antibody (Molecular Probes) for 2 h at room temperature. Sections were counterstained with DAPI and visualized by fluorescence microscopy.

6. ABBREVIATIONS

AP	Adaptor protein or Assembly polypeptide; both relate to the same complex
BFA	Brefeldin A
BSA	Bovine serum albumin
CGN	Cis-Golgi network
CNS	Central nervous system
CTxB	Cholera toxin B-subunit
DAPI	4',6-Diamidino-2-phenylindole
ER	Endoplasmic reticulum
EST	Expressed sequence tag
FITC	Fluorescein-isothiocyanate
GFP	Green fluorescent protein
GGA	Golgi-localized, γ -ear-containing, Arf-binding protein
MPR, M6PR	Mannose-6-phosphate receptor
NADPH	Reduced nicotinamide adenine dinucleotide phosphate
siRNA	Short interfering RNA
(v/t)SNARE	(vesicular/target) soluble N-ethylmaleimide-sensitive factor attachment protein receptor
PBS	Phosphate-buffered saline
PCR	Polymerase chain reaction
PKC	Protein kinase C
PNS	Postnuclear supernatant
RNAi	Ribonucleic acid-based gene interference
RNAi(VB)	Vector-based RNA interference
Tf	Transferrin
TGN	Trans-Golgi network
VSVG	G-glycoprotein of the vesicular stomatitis virus
WD	Tryptophan-Aspartic Acid (dipeptide)

7. LITERATURE

- Acharya, U., A. Mallabiabarrena, J.K. Acharya, and V. Malhotra. 1998. Signaling via mitogen-activated protein kinase kinase (MEK1) is required for Golgi fragmentation during mitosis. *Cell.* 92:183-92.
- Acharya, U., J.M. McCaffery, R. Jacobs, and V. Malhotra. 1995. Reconstitution of vesiculated Golgi membranes into stacks of cisternae: requirement of NSF in stack formation. *J Cell Biol.* 129:577-89.
- Ahle, S., and E. Ungewickell. 1989. Identification of a clathrin binding subunit in the HA2 adaptor protein complex. *J Biol Chem.* 264:20089-93.
- Aridor, M., J. Weissman, S. Bannykh, C. Nuoffer, and W.E. Balch. 1998. Cargo selection by the COPII budding machinery during export from the ER. *J Cell Biol.* 141:61-70.
- Aroian, R.V., C. Field, G. Pruliere, C. Kenyon, and B.M. Alberts. 1997. Isolation of actin-associated proteins from *Caenorhabditis elegans* oocytes and their localization in the early embryo. *Embo J.* 16:1541-9.
- Asano, S., M. Mishima, and E. Nishida. 2001. Coronin forms a stable dimer through its C-terminal coiled coil region: an implicated role in its localization to cell periphery. *Genes Cells.* 6:225-35.
- Axelsson, M.A., and G. Warren. 2004. Rapid, endoplasmic reticulum-independent diffusion of the mitotic Golgi haze. *Mol Biol Cell.* 15:1843-52.
- Barlowe, C. 2002. COPII-dependent transport from the endoplasmic reticulum. *Curr Opin Cell Biol.* 14:417-22.
- Belden, W.J., and C. Barlowe. 2001a. Distinct roles for the cytoplasmic tail sequences of Emp24p and Erv25p in transport between the endoplasmic reticulum and Golgi complex. *J Biol Chem.* 276:43040-8.
- Belden, W.J., and C. Barlowe. 2001b. Role of Erv29p in collecting soluble secretory proteins into ER-derived transport vesicles. *Science.* 294:1528-31.
- Bharathi, V., S.K. Pallavi, R. Bajpai, B.S. Emerald, and L.S. Shashidhara. 2004. Genetic characterization of the *Drosophila* homologue of coronin. *J Cell Sci.* 117:1911-22.
- Bonifacino, J.S. 2004. The GGA proteins: adaptors on the move. *Nat Rev Mol Cell Biol.* 5:23-32.
- Brown, M.R., and C.S. Chew. 1989. Carbachol-induced protein phosphorylation in parietal cells: regulation by [Ca²⁺]i. *Am J Physiol.* 257:G99-110.
- Buck, T.M., J. Eledge, and W.R. Skach. 2004. Evidence for stabilization of aquaporin-2 folding mutants by N-linked glycosylation in endoplasmic reticulum. *Am J Physiol Cell Physiol.* 287:C1292-9.
- Cai, L., N. Holowecykj, M.D. Schaller, and J.E. Bear. 2005. Phosphorylation of coronin 1B by PKC regulates interaction with ARP2/3 and cell motility. *J Biol Chem.*
- Cao, H., J.D. Orth, J. Chen, S.G. Weller, J.E. Heuser, and M.A. McNiven. 2003. Cortactin is a component of clathrin-coated pits and participates in receptor-mediated endocytosis. *Mol Cell Biol.* 23:2162-70.
- Chew, C.S., C.J. Zhou, and J.A. Parente, Jr. 1997. Ca²⁺-independent protein kinase C isoforms may modulate parietal cell HCl secretion. *Am J Physiol.* 272:G246-56.

- Colanzi, A., T.J. Deerinck, M.H. Ellisman, and V. Malhotra. 2000. A specific activation of the mitogen-activated protein kinase kinase 1 (MEK1) is required for Golgi fragmentation during mitosis. *J Cell Biol.* 149:331-9.
- Cvrckova, F., F. Rivero, and B. Bavlnka. 2004. Evolutionarily conserved modules in actin nucleation: lessons from Dictyostelium discoideum and plants. Review article. *Protoplasma*. 224:15-31.
- Da Costa, S.R., E. Sou, J. Xie, F.A. Yarber, C.T. Okamoto, M. Pidgeon, M.M. Kessels, A.K. Mircheff, J.E. Schechter, B. Qualmann, and S.F. Hamm-Alvarez. 2003. Impairing actin filament or syndapin functions promotes accumulation of clathrin-coated vesicles at the apical plasma membrane of acinar epithelial cells. *Mol Biol Cell.* 14:4397-413.
- Dascher, C., J. Matteson, and W.E. Balch. 1994. Syntaxin 5 regulates endoplasmic reticulum to Golgi transport. *J Biol Chem.* 269:29363-6.
- David, V., E. Gouin, M.V. Troys, A. Grogan, A.W. Segal, C. Ampe, and P. Cossart. 1998. Identification of cofilin, coronin, Rac and capZ in actin tails using a Listeria affinity approach. *J Cell Sci.* 111 (Pt 19):2877-84.
- de Hostos, E.L. 1999. The coronin family of actin-associated proteins. *Trends Cell Biol.* 9:345-50.
- de Hostos, E.L., B. Bradtke, F. Lottspeich, R. Guggenheim, and G. Gerisch. 1991. Coronin, an actin binding protein of Dictyostelium discoideum localized to cell surface projections, has sequence similarities to G protein beta subunits. *Embo J.* 10:4097-104.
- Dell'Angelica, E.C., J. Klumperman, W. Stoorvogel, and J.S. Bonifacino. 1998. Association of the AP-3 adaptor complex with clathrin. *Science.* 280:431-4.
- Didichenko, S.A., A.W. Segal, and M. Thelen. 2000. Evidence for a pool of coronin in mammalian cells that is sensitive to PI 3-kinase. *FEBS Lett.* 485:147-52.
- Dominguez, M., K. Dejgaard, J. Fullekrug, S. Dahan, A. Fazel, J.P. Paccaud, D.Y. Thomas, J.J. Bergeron, and T. Nilsson. 1998. gp25L/emp24/p24 protein family members of the cis-Golgi network bind both COP I and II coatomer. *J Cell Biol.* 140:751-65.
- Duncan, M.C., G. Costaguta, and G.S. Payne. 2003. Yeast epsin-related proteins required for Golgi-endosome traffic define a gamma-adaptin ear-binding motif. *Nat Cell Biol.* 5:77-81.
- Ferrari, G., H. Langen, M. Naito, and J. Pieters. 1999. A coat protein on phagosomes involved in the intracellular survival of mycobacteria. *Cell.* 97:435-47.
- Fingerhut, A., K. von Figura, and S. Honing. 2001. Binding of AP2 to sorting signals is modulated by AP2 phosphorylation. *J Biol Chem.* 276:5476-82.
- Fong, H.K., J.B. Hurley, R.S. Hopkins, R. Miake-Lye, M.S. Johnson, R.F. Doolittle, and M.I. Simon. 1986. Repetitive segmental structure of the transducin beta subunit: homology with the CDC4 gene and identification of related mRNAs. *Proc Natl Acad Sci U S A.* 83:2162-6.
- Gallione, C.J., and J.K. Rose. 1985. A single amino acid substitution in a hydrophobic domain causes temperature-sensitive cell-surface transport of a mutant viral glycoprotein. *J Virol.* 54:374-82.
- Gatfield, J., I. Albrecht, B. Zanolari, M.O. Steinmetz, and J. Pieters. 2005. Association of the leukocyte plasma membrane with the actin cytoskeleton through coiled coil-mediated trimeric coronin 1 molecules. *Mol Biol Cell.* 16:2786-98.
- Giraudo, C.G., and H.J. Maccioni. 2003. Endoplasmic reticulum export of glycosyltransferases depends on interaction of a cytoplasmic dibasic motif with Sar1. *Mol Biol Cell.* 14:3753-66.
- Gleeson, P.A., J.G. Lock, M.R. Luke, and J.L. Stow. 2004. Domains of the TGN: coats, tethers and G proteins. *Traffic.* 5:315-26.

- Goode, B.L., J.J. Wong, A.C. Butty, M. Peter, A.L. McCormack, J.R. Yates, D.G. Drubin, and G. Barnes. 1999. Coronin promotes the rapid assembly and cross-linking of actin filaments and may link the actin and microtubule cytoskeletons in yeast. *J Cell Biol.* 144:83-98.
- Grogan, A., E. Reeves, N. Keep, F. Wientjes, N.F. Totty, A.L. Burlingame, J.J. Hsuan, and A.W. Segal. 1997. Cytosolic phox proteins interact with and regulate the assembly of coronin in neutrophils. *J Cell Sci.* 110 (Pt 24):3071-81.
- Hasse, A., A. Rosentreter, Z. Spoerl, M. Stumpf, A.A. Noegel, and C.S. Clemen. 2005. Coronin 3 and its role in murine brain morphogenesis. *Eur J Neurosci.* 21:1155-68.
- Heil-Chapdelaine, R.A., N.K. Tran, and J.A. Cooper. 1998. The role of *Saccharomyces cerevisiae* coronin in the actin and microtubule cytoskeletons. *Curr Biol.* 8:1281-4.
- Hirschberg, K., C.M. Miller, J. Ellenberg, J.F. Presley, E.D. Siggia, R.D. Phair, and J. Lippincott-Schwartz. 1998. Kinetic analysis of secretory protein traffic and characterization of golgi to plasma membrane transport intermediates in living cells. *J Cell Biol.* 143:1485-503.
- Hui, N., N. Nakamura, B. Sonnichsen, D.T. Shima, T. Nilsson, and G. Warren. 1997. An isoform of the Golgi t-SNARE, syntaxin 5, with an endoplasmic reticulum retrieval signal. *Mol Biol Cell.* 8:1777-87.
- Humphries, C.L., H.I. Balcer, J.L. D'Agostino, B. Winsor, D.G. Drubin, G. Barnes, B.J. Andrews, and B.L. Goode. 2002. Direct regulation of Arp2/3 complex activity and function by the actin binding protein coronin. *J Cell Biol.* 159:993-1004.
- Iizaka, M., H.J. Han, H. Akashi, Y. Furukawa, Y. Nakajima, S. Sugano, M. Ogawa, and Y. Nakamura. 2000. Isolation and chromosomal assignment of a novel human gene, CORO1C, homologous to coronin-like actin-binding proteins. *Cytogenet Cell Genet.* 88:221-4.
- Itoh, S., K. Suzuki, J. Nishihata, M. Iwasa, T. Oku, S. Nakajin, W.M. Nauseef, and S. Toyoshima. 2002. The role of protein kinase C in the transient association of p57, a coronin family actin-binding protein, with phagosomes. *Biol Pharm Bull.* 25:837-44.
- Janvier, K., Y. Kato, M. Boehm, J.R. Rose, J.A. Martina, B.Y. Kim, S. Venkatesan, and J.S. Bonifacino. 2003. Recognition of dileucine-based sorting signals from HIV-1 Nef and LIMP-II by the AP-1 gamma-sigma1 and AP-3 delta-sigma3 hemicomplexes. *J Cell Biol.* 163:1281-90.
- Jesch, S.A., and A.D. Linstedt. 1998. The Golgi and endoplasmic reticulum remain independent during mitosis in HeLa cells. *Mol Biol Cell.* 9:623-35.
- Jokitalo, E., N. Cabrera-Poch, G. Warren, and D.T. Shima. 2001. Golgi clusters and vesicles mediate mitotic inheritance independently of the endoplasmic reticulum. *J Cell Biol.* 154:317-30.
- Li, D., and R. Roberts. 2001. WD-repeat proteins: structure characteristics, biological function, and their involvement in human diseases. *Cell Mol Life Sci.* 58:2085-97.
- Lin, C.Y., M.L. Madsen, F.R. Yarm, Y.J. Jang, X. Liu, and R.L. Erikson. 2000. Peripheral Golgi protein GRASP65 is a target of mitotic polo-like kinase (Plk) and Cdc2. *Proc Natl Acad Sci U S A.* 97:12589-94.
- Lippincott-Schwartz, J., L.C. Yuan, J.S. Bonifacino, and R.D. Klausner. 1989. Rapid redistribution of Golgi proteins into the ER in cells treated with brefeldin A: evidence for membrane cycling from Golgi to ER. *Cell.* 56:801-13.
- Lowe, M., C. Rabouille, N. Nakamura, R. Watson, M. Jackman, E. Jamsa, D. Rahman, D.J. Pappin, and G. Warren. 1998. Cdc2 kinase directly phosphorylates the cis-Golgi matrix protein GM130 and is required for Golgi fragmentation in mitosis. *Cell.* 94:783-93.

- Majoul, I., K. Sohn, F.T. Wieland, R. Pepperkok, M. Pizza, J. Hillemann, and H.D. Soling. 1998. KDEL receptor (Erd2p)-mediated retrograde transport of the cholera toxin A subunit from the Golgi involves COPI, p23, and the COOH terminus of Erd2p. *J Cell Biol.* 143:601-12.
- Majoul, I.V., P.I. Bastiaens, and H.D. Soling. 1996. Transport of an external Lys-Asp-Glu-Leu (KDEL) protein from the plasma membrane to the endoplasmic reticulum: studies with cholera toxin in Vero cells. *J Cell Biol.* 133:777-89.
- Mogelsvang, S., B.J. Marsh, M.S. Ladinsky, and K.E. Howell. 2004. Predicting function from structure: 3D structure studies of the mammalian Golgi complex. *Traffic.* 5:338-45.
- Morissette, N.S., E.S. Gold, J. Guo, J.A. Hamerman, A. Ozinsky, V. Bedian, and A.A. Aderem. 1999. Isolation and characterization of monoclonal antibodies directed against novel components of macrophage phagosomes. *J Cell Sci.* 112 (Pt 24):4705-13.
- Mundy, D.I., T. Machleidt, Y.S. Ying, R.G. Anderson, and G.S. Bloom. 2002. Dual control of caveolar membrane traffic by microtubules and the actin cytoskeleton. *J Cell Sci.* 115:4327-39.
- Nakai, K., and P. Horton. 1999. PSORT: a program for detecting sorting signals in proteins and predicting their subcellular localization. *Trends Biochem Sci.* 24:34-6.
- Nakamura, N., C. Rabouille, R. Watson, T. Nilsson, N. Hui, P. Slusarewicz, T.E. Kreis, and G. Warren. 1995. Characterization of a cis-Golgi matrix protein, GM130. *J Cell Biol.* 131:1715-26.
- Nakamura, T., K. Takeuchi, S. Muraoka, H. Takezoe, N. Takahashi, and N. Mori. 1999. A neurally enriched coronin-like protein, ClipinC, is a novel candidate for an actin cytoskeleton-cortical membrane-linking protein. *J Biol Chem.* 274:13322-7.
- Nal, B., P. Carroll, E. Mohr, C. Verthuy, M.I. Da Silva, O. Gayet, X.J. Guo, H.T. He, A. Alcover, and P. Ferrier. 2004. Coronin-1 expression in T lymphocytes: insights into protein function during T cell development and activation. *Int Immunol.* 16:231-40.
- Neer, E.J., and T.F. Smith. 1996. G protein heterodimers: new structures propel new questions. *Cell.* 84:175-8.
- Neubrand, V.E., R.D. Will, W. Mobius, A. Poustka, S. Wiemann, P. Schu, C.G. Dotti, R. Pepperkok, and J.C. Simpson. 2005. Gamma-BAR, a novel AP-1-interacting protein involved in post-Golgi trafficking. *Embo J.* 24:1122-33.
- Novina, C.D., and P.A. Sharp. 2004. The RNAi revolution. *Nature.* 430:161-4.
- Ohno, H., J. Stewart, M.C. Fournier, H. Bosshart, I. Rhee, S. Miyatake, T. Saito, A. Gallusser, T. Kirchhausen, and J.S. Bonifacino. 1995. Interaction of tyrosine-based sorting signals with clathrin-associated proteins. *Science.* 269:1872-5.
- Oku, T., S. Itoh, R. Ishii, K. Suzuki, W.M. Nauseef, S. Toyoshima, and T. Tsuji. 2005. Homotypic dimerization of the actin-binding protein p57/coronin-1 mediated by a leucine zipper motif in the C-terminal region. *Biochem J.* 387:325-31.
- Oku, T., S. Itoh, M. Okano, A. Suzuki, K. Suzuki, S. Nakajin, T. Tsuji, W.M. Nauseef, and S. Toyoshima. 2003. Two regions responsible for the actin binding of p57, a mammalian coronin family actin-binding protein. *Biol Pharm Bull.* 26:409-16.
- Okumura, M., C. Kung, S. Wong, M. Rodgers, and M.L. Thomas. 1998. Definition of family of coronin-related proteins conserved between humans and mice: close genetic linkage between coronin-2 and CD45-associated protein. *DNA Cell Biol.* 17:779-87.
- Page, L.J., P.J. Sowerby, W.W. Lui, and M.S. Robinson. 1999. Gamma-synergins: an EH domain-containing protein that interacts with gamma-adaptin. *J Cell Biol.* 146:993-1004.
- Parente, J.A., Jr., X. Chen, C. Zhou, A.C. Petropoulos, and C.S. Chew. 1999. Isolation, cloning, and characterization of a new mammalian coronin family member, coroninse, which is regulated within the protein kinase C signaling pathway. *J Biol Chem.* 274:3017-25.

- Pecot, M.Y., and V. Malhotra. 2004. Golgi membranes remain segregated from the endoplasmic reticulum during mitosis in mammalian cells. *Cell*. 116:99-107.
- Peyroche, A., B. Antonny, S. Robineau, J. Acker, J. Cherfils, and C.L. Jackson. 1999. Brefeldin A acts to stabilize an abortive ARF-GDP-Sec7 domain protein complex: involvement of specific residues of the Sec7 domain. *Mol Cell*. 3:275-85.
- Presley, J.F., N.B. Cole, T.A. Schroer, K. Hirschberg, K.J. Zaal, and J. Lippincott-Schwartz. 1997. ER-to-Golgi transport visualized in living cells. *Nature*. 389:81-5.
- Presley, J.F., T.H. Ward, A.C. Pfeifer, E.D. Siggia, R.D. Phair, and J. Lippincott-Schwartz. 2002. Dissection of COPI and Arf1 dynamics in vivo and role in Golgi membrane transport. *Nature*. 417:187-93.
- Puertollano, R., R.C. Aguilar, I. Gorshkova, R.J. Crouch, and J.S. Bonifacino. 2001a. Sorting of mannose 6-phosphate receptors mediated by the GGAs. *Science*. 292:1712-6.
- Puertollano, R., P.A. Randazzo, J.F. Presley, L.M. Hartnell, and J.S. Bonifacino. 2001b. The GGAs promote ARF-dependent recruitment of clathrin to the TGN. *Cell*. 105:93-102.
- Rabouille, C., T.P. Levine, J.M. Peters, and G. Warren. 1995. An NSF-like ATPase, p97, and NSF mediate cisternal regrowth from mitotic Golgi fragments. *Cell*. 82:905-14.
- Rappleye, C.A., A.R. Paredez, C.W. Smith, K.L. McDonald, and R.V. Aroian. 1999. The coronin-like protein POD-1 is required for anterior-posterior axis formation and cellular architecture in the nematode *caenorhabditis elegans*. *Genes Dev*. 13:2838-51.
- Ricotta, D., S.D. Conner, S.L. Schmid, K. von Figura, and S. Honing. 2002. Phosphorylation of the AP2 mu subunit by AAK1 mediates high affinity binding to membrane protein sorting signals. *J Cell Biol*. 156:791-5.
- Robinson, M.S. 2004. Adaptable adaptors for coated vesicles. *Trends Cell Biol*. 14:167-74.
- Rossanese, O.W., and B.S. Glick. 2001. Deconstructing Golgi inheritance. *Traffic*. 2:589-96.
- Rossanese, O.W., C.A. Reinke, B.J. Bevis, A.T. Hammond, I.B. Sears, J. O'Connor, and B.S. Glick. 2001. A role for actin, Cdc1p, and Myo2p in the inheritance of late Golgi elements in *Saccharomyces cerevisiae*. *J Cell Biol*. 153:47-62.
- Rothenberg, M.E., S.L. Rogers, R.D. Vale, L.Y. Jan, and Y.N. Jan. 2003. Drosophila pod-1 crosslinks both actin and microtubules and controls the targeting of axons. *Neuron*. 39:779-91.
- Rybakin, V., and C.S. Clemens. 2005. Coronin proteins as multifunctional regulators of the cytoskeleton and membrane trafficking. *Bioessays*. 27:625-32.
- Rybakin, V., M. Stumpf, A. Schulze, I.V. Majoul, A.A. Noegel, and A. Hasse. 2004. Coronin 7, the mammalian POD-1 homologue, localizes to the Golgi apparatus. *FEBS Lett*. 573:161-7.
- Sandvig, K., B. Spilsberg, S.U. Lauvral, M.L. Torgersen, T.G. Iversen, and B. van Deurs. 2004. Pathways followed by protein toxins into cells. *Int J Med Microbiol*. 293:483-90.
- Sauvonnet, N., A. Dujeancourt, and A. Dautry-Varsat. 2005. Cortactin and dynamin are required for the clathrin-independent endocytosis of gamma-c cytokine receptor. *J Cell Biol*. 168:155-63.
- Schuller, S., J. Neefjes, T. Ottenhoff, J. Thole, and D. Young. 2001. Coronin is involved in uptake of *Mycobacterium bovis* BCG in human macrophages but not in phagosome maintenance. *Cell Microbiol*. 3:785-93.
- Schulze, K.L., K. Broadie, M.S. Perin, and H.J. Bellen. 1995. Genetic and electrophysiological studies of Drosophila syntaxin-1A demonstrate its role in nonneuronal secretion and neurotransmission. *Cell*. 80:311-20.

- Shi, X., and R.M. Elliott. 2004. Analysis of N-linked glycosylation of hantaan virus glycoproteins and the role of oligosaccharide side chains in protein folding and intracellular trafficking. *J Virol.* 78:5414-22.
- Shorter, J., and G. Warren. 1999. A role for the vesicle tethering protein, p115, in the post-mitotic stacking of reassembling Golgi cisternae in a cell-free system. *J Cell Biol.* 146:57-70.
- Shorter, J., R. Watson, M.E. Giannakou, M. Clarke, G. Warren, and F.A. Barr. 1999. GRASP55, a second mammalian GRASP protein involved in the stacking of Golgi cisternae in a cell-free system. *Embo J.* 18:4949-60.
- Shupliakov, O., O. Bloom, J.S. Gustafsson, O. Kjaerulff, P. Low, N. Tomilin, V.A. Pieribone, P. Greengard, and L. Brodin. 2002. Impaired recycling of synaptic vesicles after acute perturbation of the presynaptic actin cytoskeleton. *Proc Natl Acad Sci U S A.* 99:14476-81.
- Slepnev, V.I., and P. De Camilli. 2000. Accessory factors in clathrin-dependent synaptic vesicle endocytosis. *Nat Rev Neurosci.* 1:161-72.
- Spoerl, Z., M. Stumpf, A.A. Noegel, and A. Hasse. 2002. Oligomerization, F-actin interaction, and membrane association of the ubiquitous mammalian coronin 3 are mediated by its carboxyl terminus. *J Biol Chem.* 277:48858-67.
- Springer, S., and R. Schekman. 1998. Nucleation of COPII vesicular coat complex by endoplasmic reticulum to Golgi vesicle SNAREs. *Science.* 281:698-700.
- Springer, S., A. Spang, and R. Schekman. 1999. A primer on vesicle budding. *Cell.* 97:145-8.
- Sutterlin, C., C.Y. Lin, Y. Feng, D.K. Ferris, R.L. Erikson, and V. Malhotra. 2001. Polo-like kinase is required for the fragmentation of pericentriolar Golgi stacks during mitosis. *Proc Natl Acad Sci U S A.* 98:9128-32.
- Suzuki, K., J. Nishihata, Y. Arai, N. Honma, K. Yamamoto, T. Irimura, and S. Toyoshima. 1995. Molecular cloning of a novel actin-binding protein, p57, with a WD repeat and a leucine zipper motif. *FEBS Lett.* 364:283-8.
- Terasaki, M. 2000. Dynamics of the endoplasmic reticulum and golgi apparatus during early sea urchin development. *Mol Biol Cell.* 11:897-914.
- Trucco, A., R.S. Polishchuk, O. Martella, A. Di Pentima, A. Fusella, D. Di Giandomenico, E. San Pietro, G.V. Beznoussenko, E.V. Polishchuk, M. Baldassarre, R. Buccione, W.J. Geerts, A.J. Koster, K.N. Burger, A.A. Mironov, and A. Luini. 2004. Secretory traffic triggers the formation of tubular continuities across Golgi sub-compartments. *Nat Cell Biol.* 6:1071-81.
- Votsmeier, C., and D. Gallwitz. 2001. An acidic sequence of a putative yeast Golgi membrane protein binds COPII and facilitates ER export. *Embo J.* 20:6742-50.
- Vuillier, F., G. Dumas, C. Magnac, M.C. Prevost, A.I. Lalanne, P. Oppezzo, E. Melanitou, G. Dighiero, and B. Payelle-Brogard. 2005. Lower levels of surface B-cell-receptor expression in chronic lymphocytic leukemia are associated with glycosylation and folding defects of the mu and CD79a chains. *Blood.* 105:2933-40.
- Waguri, S., F. Dewitte, R. Le Borgne, Y. Rouille, Y. Uchiyama, J.F. Dubremetz, and B. Hoflack. 2003. Visualization of TGN to endosome trafficking through fluorescently labeled MPR and AP-1 in living cells. *Mol Biol Cell.* 14:142-55.
- Watson, P., R. Forster, K.J. Palmer, R. Pepperkok, and D.J. Stephens. 2005. Coupling of ER exit to microtubules through direct interaction of COPII with dynactin. *Nat Cell Biol.* 7:48-55.
- Wein, G., M. Rossler, R. Klug, and T. Herget. 2003. The 3'-UTR of the mRNA coding for the major protein kinase C substrate MARCKS contains a novel CU-rich element interacting with the mRNA stabilizing factors HuD and HUR. *Eur J Biochem.* 270:350-65.

- Weitzdoerfer, R., N. Gerstl, D. Pollak, H. Hoeger, W. Dreher, and G. Lubec. 2004. Long-term influence of perinatal asphyxia on the social behavior in aging rats. *Gerontology*. 50:200-5.
- Wu, M.N., T. Fergestad, T.E. Lloyd, Y. He, K. Broadie, and H.J. Bellen. 1999. Syntaxin 1A interacts with multiple exocytic proteins to regulate neurotransmitter release in vivo. *Neuron*. 23:593-605.
- Wujek, P., E. Kida, M. Walus, K.E. Wisniewski, and A.A. Golabek. 2004. N-glycosylation is crucial for folding, trafficking, and stability of human tripeptidyl-peptidase I. *J Biol Chem*. 279:12827-39.
- Yan, M., R.F. Collins, S. Grinstein, and W.S. Trimble. 2005. Coronin-1 function is required for phagosome formation. *Mol Biol Cell*. 16:3077-87.
- Yarar, D., C.M. Waterman-Storer, and S.L. Schmid. 2005. A dynamic actin cytoskeleton functions at multiple stages of clathrin-mediated endocytosis. *Mol Biol Cell*. 16:964-75.
- Yu, L., C. Gaitatzes, E. Neer, and T.F. Smith. 2000. Thirty-plus functional families from a single motif. *Protein Sci*. 9:2470-6.
- Zaal, K.J., C.L. Smith, R.S. Polishchuk, N. Altan, N.B. Cole, J. Ellenberg, K. Hirschberg, J.F. Presley, T.H. Roberts, E. Siggia, R.D. Phair, and J. Lippincott-Schwartz. 1999. Golgi membranes are absorbed into and reemerge from the ER during mitosis. *Cell*. 99:589-601.
- Zaphiropoulos, P.G., and R. Toftgard. 1996. cDNA cloning of a novel WD repeat protein mapping to the 9q22.3 chromosomal region. *DNA Cell Biol*. 15:1049-56.
- Zhang, T., and W. Hong. 2001. Ykt6 forms a SNARE complex with syntaxin 5, GS28, and Bet1 and participates in a late stage in endoplasmic reticulum-Golgi transport. *J Biol Chem*. 276:27480-7.

ABSTRACT

Coronins constitute an evolutionarily conserved family of WD-repeat actin-binding proteins, which can be clearly classified into two distinct groups based on their structural features. All coronins possess a conserved basic N-terminal motif and three to ten WD repeats clustered in one or two core domains. *Dictyostelium* and mammalian coronins are important regulators of the actin cytoskeleton, while the fly Dpod1 and the yeast coronin proteins crosslink both actin and microtubules. Apart from that, several coronins have been shown to be involved in vesicular transport. *C. elegans* POD-1 and *Drosophila* coro regulate the actin cytoskeleton, but also govern vesicular trafficking as indicated by mutant phenotypes. In both organisms, defects in cytoskeleton and trafficking lead to severe developmental defects ranging from abnormal cell division to aberrant formation of morphogen gradients.

Crn7 is a ubiquitous mammalian coronin family member. The protein is distributed between the cytosol and Golgi, where it is present at the outer side of the membrane. Golgi localization of Crn7 depends on tyrosine phosphorylation and the integrity of ER-to-Golgi transport. The protein intimately associates with the Golgi membrane and does not require coatomer for its localization. Crn7 is an essential protein, as its knockdown by RNAi leads to a dramatic time- and concentration-dependent decrease in cell viability. Crn7 RNAi cells display scattered Golgi morphology, as demonstrated by electron and light microscopy. Most importantly, the knockdown leads to the block of protein export from the Golgi complex, while the import into the organelle, both anterograde and retrograde, remains unaffected. Further, I established that Crn7 interacts with AP-1 adaptor protein complex participating in the Golgi export by linking cargoes to the clathrin coat.

The Golgi complex is the central protein sorting organelle in eukaryotic cells. The Golgi architecture varies significantly between species and cell types, but the organelle executes principally the same function. Upon the cargo protein entry from the endoplasmic reticulum, resident Golgi enzymes modify the cargo in a way that proteins destined to take different transport routes can be biochemically distinguished between and selectively recruited to the corresponding export carriers. We suggest that Golgi-localized Crn7 can function by regulating the cargo export from the Golgi, and thus affect protein sorting and trafficking along the biosynthetic pathway. We anticipate that Crn7 is recruited to the Golgi membranes by cytosolic portions of non-YxxΦ cargoes and cargo proteins, and interacts with AP-1 to allow the Golgi export of such cargoes/receptors.

ZUSAMMENFASSUNG

Die Coronine stellen eine evolutionär konservierte Proteinfamilie innerhalb der Aktin-bindenden WD-Repeat Proteine dar. Sie können aufgrund ihrer Struktureigenschaften in zwei Gruppen eingeteilt werden. Alle Coronine besitzen ein konserviertes basisches N-terminales Motiv und drei bis zehn WD-Repeats, die in einer oder zwei Zentraldomänen angeordnet sind. Coronine aus Dictyostelium und Säugetieren sind wichtige Regulatoren des Aktin-Zytoskelettes, wohingegen Dpod1 aus Drosophila und Coronin der Hefe Aktin-Filamente mit Mikrotubuli verknüpfen. Darüberhinaus wurde gezeigt, dass verschiedene Coronine eine Rolle im Vesikeltransport spielen. POD-1 aus C. elegans und Coro aus Drosophila regulieren sowohl das Aktin-Zytoskelett als auch den Vesikeltransport, wie in Mutanten gezeigt werden konnte. In beiden Organismen führen Defekte in Zytoskelett und Vesikeltransport zu schweren Entwicklungsstörungen in Form von abnormaler Zellteilung bis hin zu Abweichungen in der Bildung von morphogenetischen Gradienten.

Crn7 ist ein in Säugetieren ubiquitär vorkommendes Coronin. Das Protein ist in Zytosol und Golgi-Apparat lokalisiert, wobei es an die Außenseite der Golgi-Membranen bindet. Die Lokalisation von Crn7 an Golgi-Membranen hängt ab von Tyrosinphosphorylierung wie auch der Integrität des Vesikeltransports vom ER zum Golgi-Apparat. Crn7 bindet mit hoher Affinität an Golgi-Membranen, ohne dafür COP-Adaptorproteine zu benötigen. Dass Crn7 ein essentielles Protein ist, zeigen RNAi-Experimente, die Zeit- und Konzentrationsabhängig zu einer sehr deutlichen Verminderung des Zellüberlebens führen. Zellen, die mit siRNA gegen Crn7 behandelt werden, zeigen eine ungeordnete Golgi-Morphologie, die mittels Licht- und Elektronenmikroskopie nachgewiesen wurde. Insbesondere führt die Herunterregulation von Crn7 zu einer Blokade des allgemeinen Proteinexports aus dem Golgi-Komplex, wohingegen der Import in diese Organelle, sowohl anterograd als auch retrograd, unverändert bleibt. Darüberhinaus interagiert Crn7 mit dem AP-1 Adaptorproteinkomplex, der eine zentrale Rolle in Golgi-Exportprozessen hat, indem er die zum Export bestimmten Proteine mit Clathrin verbindet.

Der Golgi-Komplex ist die zentrale proteinsortierende Organelle. Die Architektur des Golgi-Apparates variiert deutlich zwischen den Spezies und Zelltypen, wobei sie aber grundsätzlich die gleiche Funktion erfüllt. Wird ein Protein aus dem ER in den Golgi-Apparat transportiert, wird es von Golgi-Enzymen so modifiziert, dass Proteine, die für unterschiedliche Transportwege bestimmt sind, effektiv unterschieden und für die entsprechenden Exportvesikel rekrutiert werden können. Wir stellten fest, dass das Golgi-lokalierte Crn7 eine Funktion in der Regulation des Exportes von Transitproteinen hat. Dadurch wird der anterograde biosynthetische Transport in der späten Golgi-Phase unterbrochen. Wir nehmen an, dass Crn7 durch zytosolische Anteile von nicht-YxxΦ Transitproteinen und ihren Rezeptoren an die Golgi-Membran gebunden wird und dort mit AP-1 interagiert, sodass der Export solcher Transitproteine/Rezeptoren ermöglicht wird.

ERKLÄRUNG

Ich versichere, dass ich die von mir vorgelegte Dissertation selbständig angefertigt, die benutzten Quellen und Hilfsmittel vollständig angegeben und die Stellen der Arbeit- einschließlich Tabellen und Abbildungen-, die anderen Werke im Wortlaut oder dem Sinn nach entnommen sind, in jedem Einzelfall als Entlehnung kenntlich gemacht habe; dass diese Dissertation noch keiner anderen Fakultät oder Universität zur Prüfung vorgelegen hat; dass sie - abgesehen von unten angegebenen Teilpublikationen noch nicht veröffentlicht ist, sowie, dass ich eine Veröffentlichung vor Abschluss des Promotionsverfahrens nicht vornehmen werde. Die Bestimmungen dieser Promotionsordnung sind mir bekannt. Die von mir vorgelegte Dissertation ist von Frau Prof. Dr. Angelika A. Noegel betreut worden.

Köln, 20/09/2005

Vasily Rybakin

Teilpublikationen:

Rybakin V., Gounko N., Majoul I.V., Duden, R., Noegel, A.A. Crn7 is a putative adaptor required for the Golgi export in mammalian cells. *Submitted*.

Rybakin V., Clemen C.S. Coronin proteins as multifunctional regulators of the cytoskeleton and membrane trafficking. *Bioessays*. 2005 Jun;27(6):625-32.

Rybakin V., Stumpf M., Schulze A., Majoul I.V., Noegel A.A., Hasse A. Coronin 7, the mammalian POD-1 homologue, localizes to the Golgi apparatus. *FEBS Lett.* 2004 Aug 27;573(1-3):161-7.

CURRICULUM VITAE

Name: Vasily Rybakin
Address : Gleueler Str. 229, 50935 Köln
Address (home country): Tikhoretski 31/1-63, St. Petersburg, 195427 Russland
E-mail: iznakurnozh@yahoo.com
Date of Birth: 29.05.1978
Nationality: Russian

School studies

1985-1993: School 514, St. Petersburg, Russia
1993-1995: School 45, St. Petersburg, Russia (Abitur)

University studies

1995-2000: Bachelor of Science (Biology), Honours degree;
University of St. Petersburg, Russia

2000-2002: Master of Science (Immunology), Honours degree;
Dept. of Cell Biology,
University of St. Petersburg, Russia

Doctoral studies

09.2002 - 09.2005: PhD fellowship financed by the Graduate School in Genetics
and Functional Genomics, University of Cologne

04.2003 - 11.2005: PhD Thesis work:
Institute for Biochemistry I
Faculty of Mathematics and Natural Science
University of Cologne
Supervisor: Prof. Dr. Angelika A. Noegel

LEBENSLAUF

Name: Vasily Rybakin
Adresse : Gleueler Str. 229, 50935 Köln
Heimatadresse: Tikhoretski 31/1-63, St. Petersburg, 195427 Russland
E-mail: iznakurnozh@yahoo.com
Geburtsdatum: 29.05.1978
Staatsangehörigkeit: Russisch

Schulausbildung

1985-1993: Schule 514, St. Petersburg, Russland
1993-1995: Schule 45, St. Petersburg, Russland (Abitur)

Hochschulausbildung

1995-2000: Bachelor of Science (Biologie)
Universität St. Petersburg, Russland

2000-2002: Master of Science (Immunologie)
Abt. Zellbiologie
Universität St. Petersburg, Russland

Promotion

09.2002 - 09.2005: Stipendiat bei der Graduate School in Genetics and Functional Genomics", Universität zu Köln.

04.2003 - 11.2005: Promotionsarbeit:
Institut für Biochemie I
Mathematisch-Naturwissenschaftliche Fakultät
Universität zu Köln
Betreuerin: Prof. Dr. Angelika A. Noegel